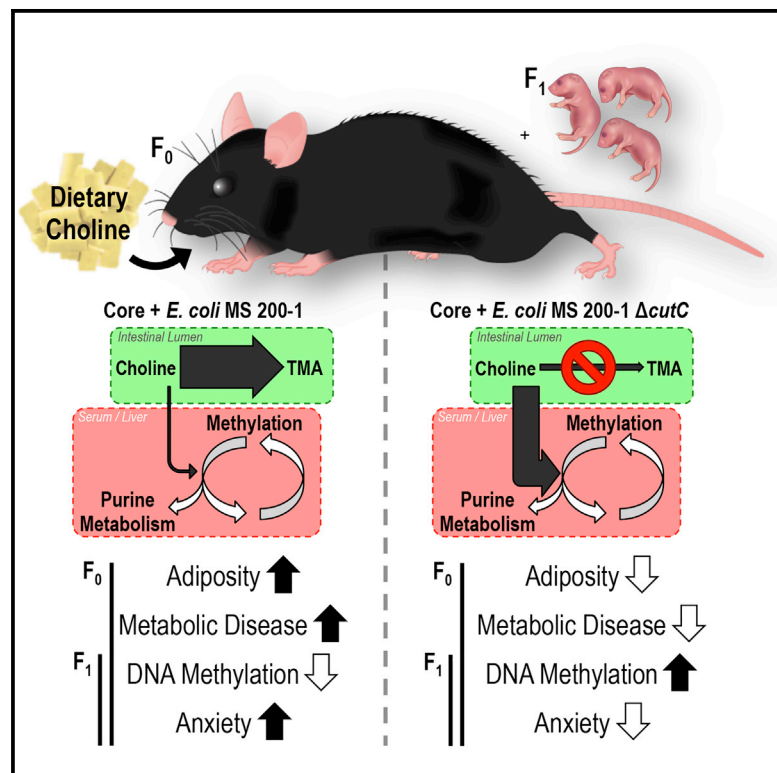


# Cell Host & Microbe

## Metabolic, Epigenetic, and Transgenerational Effects of Gut Bacterial Choline Consumption

### Graphical Abstract



### Authors

Kymerleigh A. Romano,  
Ana Martinez-del Campo,  
Kazuyuki Kasahara, ...,  
Daniel Amador-Noguez,  
Emily P. Balskus, Federico E. Rey

### Correspondence

balskus@chemistry.harvard.edu (E.P.B.),  
ferey@wisc.edu (F.E.R.)

### In Brief

The gut microbiota is a dynamic metabolic organ associated with host health and disease phenotypes. Romano, Martinez-del Campo et al. report that choline-consuming gut bacteria reduce the bioavailability of this essential nutrient and deplete methyl-donor metabolites, resulting in alterations to host epigenetic programming and increased susceptibility to metabolic disease.

### Highlights

- Gut bacteria compete with the host for choline, decreasing bioavailability
- Microbial choline degradation depletes methyl-donor metabolites
- Microbial choline utilization alters in utero epigenetic programming of the brain
- Mice with choline-consuming gut microbiota display altered behavior



# Metabolic, Epigenetic, and Transgenerational Effects of Gut Bacterial Choline Consumption

Kymerleigh A. Romano,<sup>1,3</sup> Ana Martinez-del Campo,<sup>2,3</sup> Kazuyuki Kasahara,<sup>1</sup> Carina L. Chittim,<sup>2</sup> Eugenio I. Vivas,<sup>1</sup> Daniel Amador-Nogues,<sup>1</sup> Emily P. Balskus,<sup>2,4,\*</sup> and Federico E. Rey<sup>1,4,5,\*</sup>

<sup>1</sup>Department of Bacteriology, University of Wisconsin-Madison, Madison, WI 53706, USA

<sup>2</sup>Department of Chemistry and Chemical Biology, Harvard University, Cambridge, MA 02138, USA

<sup>3</sup>These authors contributed equally

<sup>4</sup>Senior author

<sup>5</sup>Lead Contact

\*Correspondence: [balskus@chemistry.harvard.edu](mailto:balskus@chemistry.harvard.edu) (E.P.B.), [ferey@wisc.edu](mailto:ferey@wisc.edu) (F.E.R.)

<http://dx.doi.org/10.1016/j.chom.2017.07.021>

## SUMMARY

Choline is an essential nutrient and methyl donor required for epigenetic regulation. Here, we assessed the impact of gut microbial choline metabolism on bacterial fitness and host biology by engineering a microbial community that lacks a single choline-utilizing enzyme. Our results indicate that choline-utilizing bacteria compete with the host for this nutrient, significantly impacting plasma and hepatic levels of methyl-donor metabolites and recapitulating biochemical signatures of choline deficiency. Mice harboring high levels of choline-consuming bacteria showed increased susceptibility to metabolic disease in the context of a high-fat diet. Furthermore, bacterially induced reduction of methyl-donor availability influenced global DNA methylation patterns in both adult mice and their offspring and engendered behavioral alterations. Our results reveal an underappreciated effect of bacterial choline metabolism on host metabolism, epigenetics, and behavior. This work suggests that interpersonal differences in microbial metabolism should be considered when determining optimal nutrient intake requirements.

## INTRODUCTION

Choline is a quaternary amine required for many biological processes including maintenance of the structural integrity of cell membranes and support of cholinergic neurotransmission. Additionally, choline provides one-carbon units for the synthesis of the ubiquitous methyl donor *S*-adenosylmethionine (SAM). Long-term dietary choline deficiency results in substantial alterations to epigenetic regulation such as DNA methylation (Pogribny and Beland, 2009). Changes in DNA methylation have been associated with various human pathologies, including cancer, aging, atherosclerosis, cognitive disabilities (such as depression, anxiety, schizophrenia, or Alzheimer's disease), and autoimmune disorders (Pogribny and Beland, 2009). Furthermore, choline

plays an important role in lipid metabolism, as it is required for the assembly/secretion of very-low-density lipoproteins (VLDL) (Fungwe et al., 1992). Despite choline's high abundance in common dietary constituents, it is estimated that only 10% of the United States population consistently meets or exceeds the daily recommended intake of this essential nutrient established by the Institute of Medicine (Zeisel and da Costa, 2009).

The demand for choline increases during pregnancy and lactation: choline levels in amniotic fluid are 14-fold higher than in maternal plasma, and circulating levels of choline in infants are higher than in adults (Ozarda Ilcol et al., 2002; McMahon and Farrell, 1985). During gestation, maternal choline deficiency reduces global DNA methylation in the fetal hippocampus and alters the development and function of cholinergic neurons that participate in learning, memory, and attention (Mellott et al., 2007; Zeisel, 2007). A recent study showed that perinatal phosphatidylcholine supplementation (above current standards) is associated with less social withdrawal and fewer attention-deficit problems in ~3-year-old children compared to an age-matched placebo group (Ross et al., 2016). Remarkably, it is estimated that 90%–95% of pregnant women fail to meet the minimum recommended levels of choline intake (Brunst et al., 2014).

While choline does not compete with other nutrients for enterocyte transport, previous evidence suggests that gut microbes can limit its bioavailability (Romano et al., 2015). Gut bacterial choline metabolism generates trimethylamine (TMA) via a recently identified pathway (Craciun and Balskus, 2012). The choline utilization (*cut*) gene cluster encodes the glycy radical enzyme choline TMA-lyase (CutC), which converts choline into TMA and acetaldehyde under anaerobic conditions. Culture-based and metagenomic studies have revealed a wide distribution of the *cut* pathway among bacteria and indicate it represents a major pathway for microbial choline utilization in the human intestine (Chen et al., 2016; Falony et al., 2015; Martínez-del Campo et al., 2015; Romano et al., 2015).

TMA produced in the intestinal lumen is absorbed into the bloodstream and further metabolized in the liver to trimethylamine-*N*-oxide (TMAO) by host flavin monooxygenase enzymes (Baker and Chaykin, 1962). Human studies have revealed that high serum levels of TMAO are positively associated with impaired renal function, non-alcoholic fatty liver disease (NAFLD), cardiovascular disease (CVD), and diabetes (Dambrova et al., 2016;

Koeth et al., 2013; Tang et al., 2015; Wang et al., 2011). Additionally, a recent study in Malawian children showed linear growth failure and impaired cognitive function associated with low serum choline and high TMAO-to-choline ratios (Semba et al., 2016).

Despite recent progress made in characterizing the impact of TMAO on the host, there have not been studies that comprehensively evaluate the functional consequences of gut microbial “removal” of choline in healthy or diseased states. Specifically, it is not clear whether choline consumption by gut bacteria impacts host methyl-donor availability and the multiple metabolic processes that depend on this nutrient. Here, we develop an experimental framework for addressing these questions by establishing a gnotobiotic mouse model harboring a synthetic gut bacterial community in which choline utilization can be manipulated. Using this model, we discovered that choline-utilizing bacteria effectively compete with the host for this nutrient and lower bioavailability of methyl-donor metabolites. We then explored the potential implications of this finding on two health conditions that are highly sensitive to methyl-donor availability: high-fat (HF) diet-induced metabolic disease (Craig, 2004) and pregnancy/early life (Zeisel, 2006). We found that bacterially induced depletion of metabolites involved in one-carbon metabolism results in increased susceptibility to metabolic disease and alters epigenetic regulation across multiple tissues, including the fetal brain.

## RESULTS

### Identification of a Choline Utilization Gene Cluster in *E. coli* MS 200-1, a Human Gastrointestinal Isolate

Previous analyses uncovered *cut* gene clusters in a subset of species within the Enterobacteriaceae, including 94 *E. coli* strains (Martinez-del Campo et al., 2015). A more recent BLAST search identified an additional 164 *E. coli* strains that carry these genes. The large majority (~96%) of these *cut* gene cluster-containing isolates are from the human urogenital tract, gastrointestinal tract, or bloodstream (Figure 1A). Only 4% of sequenced *E. coli* genomes have a *cut* gene cluster, indicating that these genes are part of this organism’s open and continuously evolving pangenome.

*E. coli* MS 200-1, a human gut strain that was isolated from the ileum of a patient with normal histology, was chosen for genetic characterization of the *cut* gene cluster due to its genetic tractability and ability to robustly colonize the small intestine, which is the primary site of choline absorption. This strain possesses a “type II” *cut* gene cluster (Figure 1B), which contains fewer total genes compared to the “type I” *cut* gene cluster originally described in the  $\delta$ -proteobacterium *Desulfovibrio desulfuricans* (Craciun and Balskus, 2012). Type II *cut* gene clusters appear to encode all the proteins required for anaerobic choline metabolism, including choline trimethylamine-lyase and its activase (CutC and CutD), five putative bacterial microcompartment (BMC) structural proteins (CutN1, CutN2, CutN3, CutN4, and CutK), a coenzyme A (CoA)-acylating aldehyde oxidoreductase (CutF), an alcohol dehydrogenase (CutO), and a phosphotransacetylase (CutH) (Figure 1C). We inspected the genetic context of the *cut* gene clusters from different  $\gamma$ -proteobacteria and identified additional genes potentially involved in choline utilization, including two genes encoding predicted transcriptional regulators (*reg1* and *reg2*), two genes encoding putative small multi-

drug resistance (SMR) proteins (*SMR1* and *SMR2*), and two genes encoding conserved hypothetical proteins (*hyp1* and *hyp2*). These genes are largely conserved in  $\gamma$ -proteobacterial *cut* gene clusters but are absent from type I *cut* gene clusters found predominantly in Firmicutes, Actinobacteria, and  $\delta$ -proteobacteria.

Three of these genes can be assigned roles in choline metabolism. Reg1 is a transcriptional regulator from the TetR family that contains a BetI domain. BetI is a repressor of the *bet* (betaine) regulon, which encodes the enzymes that convert choline into glycine betaine. In the absence of choline, BetI represses the expression of the *bet* genes (Lamark et al., 1996). Similarly, Reg1 could be a transcriptional repressor of the *cut* pathway, which is induced when choline is present in the environment. However, the presence of a second transcriptional regulator (encoded by *reg2*) containing a helix-turn-helix DNA-binding domain suggests that the regulation of the *cut* gene cluster could be more complex than the *bet* regulon. SMR proteins act as transporters that confer resistance to quaternary cation compounds via proton motive force-energized efflux (Bay and Turner, 2012). EmrE, the best-characterized SMR protein member, transports a variety of drugs as well as choline and betaine, which are proposed to be its natural substrates. SMR1 and SMR2 could therefore encode *cut* pathway-specific transporters.

### Genetic Manipulation of Choline TMA-Lyase and Its Activase

To confirm the involvement of the *cut* gene cluster from *E. coli* MS 200-1 in anaerobic choline degradation, we constructed in-frame deletion mutants of the *cutC* and *cutD* genes, which encode choline trimethylamine-lyase and its associated radical SAM activating protein. The ability of the resulting strains to grow using choline as the carbon source under anaerobic conditions with fumarate as a terminal electron acceptor was assessed. Both knockout mutants failed to grow on choline-containing minimal medium (Figure 1D), establishing their essential role in anaerobic choline metabolism. Growth curve analyses showed the phenotypes described above could be restored by the individual expression of each wild-type (WT) gene from an IPTG inducible vector (Figure 1D).

We used liquid chromatography-mass spectroscopy (LC-MS) assays to investigate whether the *cutC* and *cutD* mutants were impaired in their ability to produce TMA when incubated in choline-containing minimal media. As shown in Figure 1E, conversion of  $d_9$ -choline into  $d_9$ -TMA was abolished in both knockouts and was restored by expression of the corresponding WT allele from a plasmid. Altogether these results validate the importance of *cutC* and *cutD* for anaerobic choline metabolism and TMA production in *E. coli*.

### Respiratory Electron Acceptors Support Anaerobic Choline Growth In Vitro

We examined whether various electron acceptors could support anaerobic growth on choline. Choline-containing minimal media supplemented with different electron acceptors were inoculated with the WT strain. Fumarate, nitrate, DMSO, and TMAO were all able to support anaerobic growth on choline (Figure 1F). In contrast, tetrathionate, the only electron acceptor used during

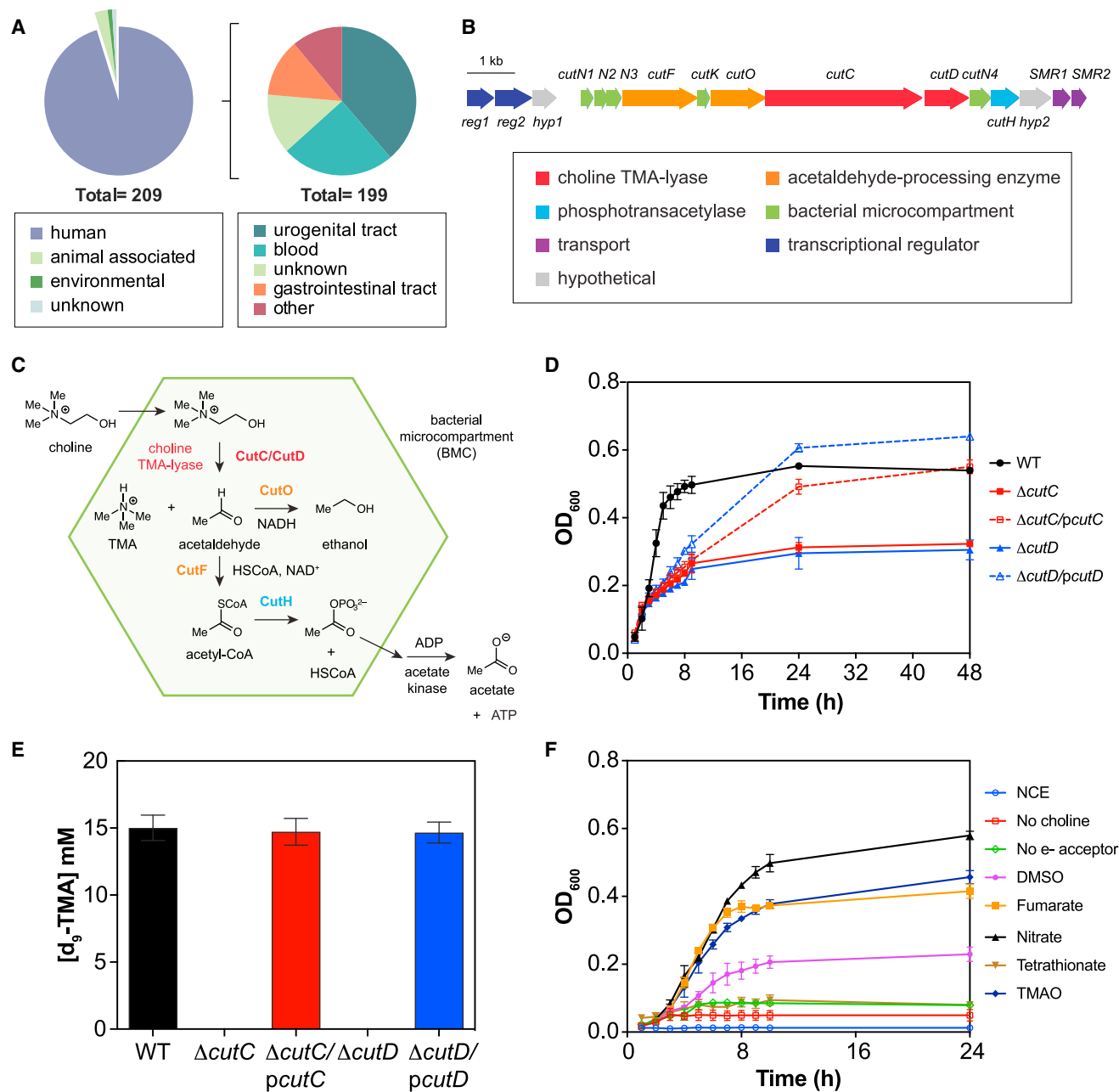


**Figure 1. In Vitro Characterization of *E. coli* MS 200-1 WT Strain and Variants Bearing *cut* Gene Cluster Mutations**

(A) Environmental distribution of sequenced *cut* gene cluster-containing *E. coli* genomes.

(B) Content and organization of the *cut* gene cluster from *E. coli* MS 200-1.

(C) Proposed model for anaerobic choline utilization.

(D) Growth phenotype of WT,  $\Delta cutC$ , and  $\Delta cutD$  strains on choline-containing minimal medium. Cells were grown by anaerobic respiration in NCE medium supplemented with 15 mM choline, 40 mM fumarate, and 0.5 mM glucose to stimulate growth.

(E) LC-MS quantification of d<sub>9</sub>-TMA produced by WT and *cut* variants in minimal medium containing 15 mM d<sub>9</sub>-choline, 40 mM fumarate, and 0.5 mM glucose. Deletions were complemented by plasmid-based inducible expression of the corresponding WT gene (designated *pcutC* and *pcutD*) by addition of 1  $\mu$ M IPTG.

(F) Anaerobic respiration of choline by *E. coli* MS 200-1 utilizing different electron acceptors. Growth curves were performed in minimal media supplemented with 15 mM choline plus 40 mM of the indicated electron acceptor.

All values are averages  $\pm$  SEMs of three independent experiments.

anaerobic respiration of ethanolamine and propanediol (closely related pathways) in *Salmonella enterica* serotype Typhimurium (Price-Carter et al., 2001), did not support anaerobic growth.

This finding is supported by the absence of homologs of the *ttr* operon in the *E. coli* MS 200-1 genome and the presence of genes that encode nitrate reductases, S-oxide reductases, and

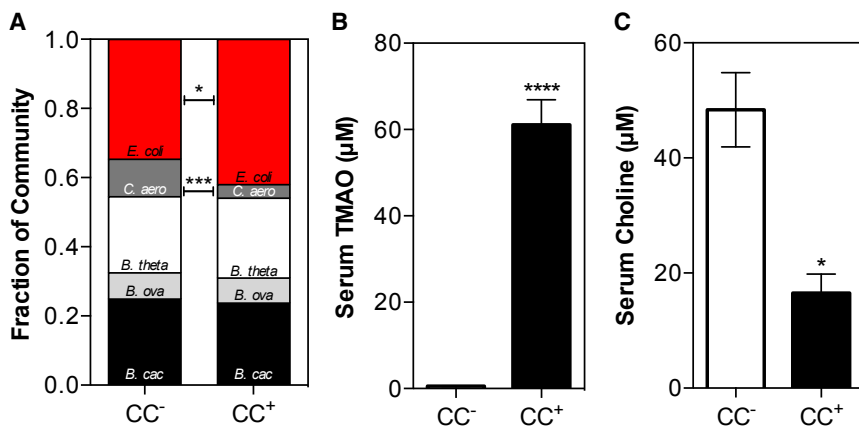


**Figure 2. In Vivo Fitness and Functional Assessment of *E. coli* MS 200-1 Choline Utilization-Deficient Mutants**

C57BL/6 females (five animals in each group) were colonized with the following microbial core community: *B. caccae*, *B. ovatus*, *B. theta*, *thetaomicron*, *C. aerofaciens*, and *E. rectale*. In addition to these five species, mice were co-colonized with either the WT *E. coli* MS 200-1 strain (CC<sup>+</sup>) or the  $\Delta cutC$  (choline trimethylamine-lyase) bearing variant (CC<sup>-</sup>). Mice were maintained for 2 weeks on a 1% (w/w) choline diet.

(A) Community profiling by sequencing (COPRO-seq) analysis of core community members and *E. coli* in cecal contents.

(B) Serum levels of TMAO.

(C) Serum levels of choline.

All values are averages  $\pm$  SEMs. Values that are significantly different (Student's *t* test) are indicated: \**p* < 0.05; \*\*\**p* < 0.001; \*\*\*\**p* < 0.0001.

*N*-oxide reductases. It has been recently demonstrated in mice that nitrate generated through the inflammatory response in the gut can be used by *E. coli* as a substrate for anaerobic respiration, allowing them to outcompete fermentative bacteria (Winter et al., 2013). We thus hypothesize that strains able to couple nitrate respiration with choline consumption may have a competitive advantage in the inflamed gut.

### Choline Utilization Provides a Moderate Fitness Advantage to *E. coli* MS 200-1 In Vivo

To assess the impact of microbial choline utilization on bacterial colonization and host biology, two groups of adult germ-free (GF) female C57BL/6 mice were colonized with the following microbial mixture: *Bacteroides caccae*, *Bacteroides ovatus*, *Bacteroides thetaiotaomicron*, *Colinsella aerofaciens*, and *Eubacterium rectale*. These organisms were selected because they are dominant members of the human gut and do not produce TMA from choline (Qin et al., 2010; Romano et al., 2015). In addition to these five species (from here on referred to as the “core community”), the mixture contained either the WT *E. coli* MS 200-1 strain (from here on referred to as “choline consuming” community, CC<sup>+</sup>) or the *E. coli* MS 200-1  $\Delta cutC$  strain, which is unable to consume choline and produce TMA (referred to as CC<sup>-</sup>). All mice were fed a purified diet containing a relatively high choline content (1% w/w choline; Envigo TD.140179) for 2 weeks after colonization. Although both *E. coli* strains colonized the intestinal tract, deletion of the *cutC* gene moderately but significantly impaired colonization compared to the WT *E. coli* strain (Figure 2A; 34.6%  $\pm$  5.0% versus 42.0%  $\pm$  4.1%, respectively). Additionally, the presence of a functional *cut* pathway negatively affected *C. aerofaciens* abundance, which colonized to significantly lower levels in the presence of the TMA-producing strain (Figure 2A). These results suggest that choline metabolism provides a fitness advantage to *E. coli* and that choline consumption and/or TMA production impacts gut community structure. Analysis of serum samples from these mice confirmed that only mice colonized with the CC<sup>+</sup> community accumulated TMAO (Figure 2B). These mice also exhibited a 3-fold reduction in serum choline (Figure 2C). These results suggest that bacterial choline consumption decreases choline bioavailability to the host.

### Bacterial Choline Utilization Recapitulates Biochemical Signatures of Diet-Induced Choline Deficiency

Choline is an important precursor for the synthesis of methionine and ultimately the methyl donor SAM. Furthermore, choline and SAM are metabolically linked with purine and creatine biosynthesis, as well as the transsulfuration pathway (Figure 3A). We investigated whether the presence of intestinal microbial choline utilization altered serum and hepatic levels of metabolites involved in one-carbon, transsulfuration, and purine metabolism in the CC<sup>+</sup> and CC<sup>-</sup> mice discussed above using untargeted metabolomics. We found that serum levels of metabolites involved in the generation of SAM, including choline, betaine, methionine, dimethylglycine, and methionine sulfoxide, were significantly reduced in the mice colonized with the CC<sup>+</sup> community (Figure 3B). Additionally, metabolites from the transsulfuration pathway, including cysteine and glutathione, were significantly increased while those associated with purine metabolism, including inosine, hypoxanthine, xanthine, kynurenine, and uric acid, were significantly reduced (Figures 3C and 3D). Synthesis of creatine requires a large amount of methyl groups (Mudd and Poole, 1975), and creatine supplementation prevents the hepatic consequences of a choline-deficient diet (Deminice et al., 2015). However, we found that creatine levels are higher in serum of CC<sup>+</sup> colonized mice compared with the CC<sup>-</sup> group (Figure 3B). While choline deficiency may impair creatine synthesis, impaired renal function can significantly increase its concentration in serum. Interestingly, TMAO, which is increased in the CC<sup>+</sup> community (Figure 2B), is associated with renal insufficiency, chronic kidney disease, and necrosis (Tang et al., 2015).

Analyses of liver metabolites revealed similar differences between the two groups of mice, including lower levels of betaine, methionine, and purine metabolites in mice colonized with the CC<sup>+</sup> community (Figures S1A and S1B). CDP-choline, an intermediate in the de novo production of phosphatidylcholine from choline (Kennedy and Weiss, 1956), was also detected at lower levels in the CC<sup>+</sup> mice (Figure S1C). During choline deficiency, hepatocytes overproduce reactive oxygen species (ROS) due to abnormal mitochondrial function and inhibition of complex I, which can lead to the signaling of apoptosis (Zeisel, 2012). Mitochondrial ROS production stimulates the transsulfuration pathway and early

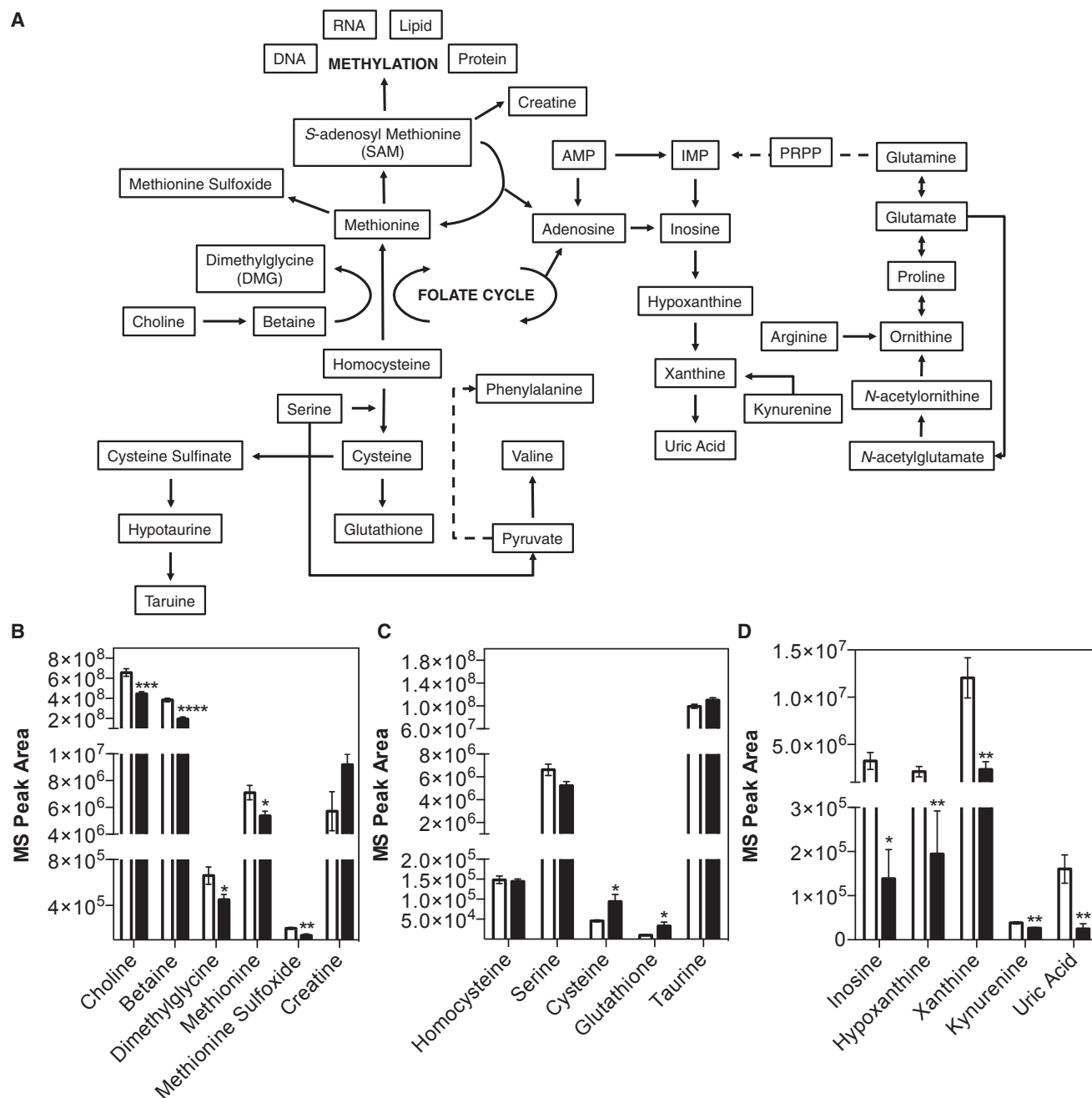


**Figure 3. Analysis of One-Carbon, Transsulfuration, and Purine Metabolism**

Measurements of serum metabolites from adult female mice colonized with either the CC<sup>-</sup> (white bars) or CC<sup>+</sup> (black bars) community maintained on a 1% choline diet were conducted using ultra-high-pressure liquid chromatography-tandem mass spectrometry (uHPLC-MS/MS) (five animals in each experimental group).

(A) Choline metabolism pathway schematic.

(B–D) Serum levels of metabolites involved in (B) one-carbon metabolism, (C) transsulfuration pathway, and (D) purine metabolism.

All values are averages ± SEMs. Values that were significantly different (Student's *t* test) are indicated: \**p* < 0.05; \*\**p* < 0.01; \*\*\**p* < 0.001; \*\*\*\**p* < 0.0001.

release of internal glutathione stores (Bhandary et al., 2012). We quantified metabolites associated with the transsulfuration pathway (Figure S1D) and found significantly higher levels of glutathione in the livers of mice colonized with the CC<sup>+</sup> community (Figure S1E). Moreover, differential expression of genes associated with ROS production and apoptosis was observed in the livers of

mice colonized with the CC<sup>+</sup> community (Table S1). As mentioned above, choline deficiency is known to impair mitochondrial function by specifically inhibiting complex I. We observed significantly reduced expression of *Ndufb2*, a complex I NADH dehydrogenase (Table S1). Reduced *Ndufb2* expression was accompanied by a simultaneous increase in NADH levels (Figure S1F).

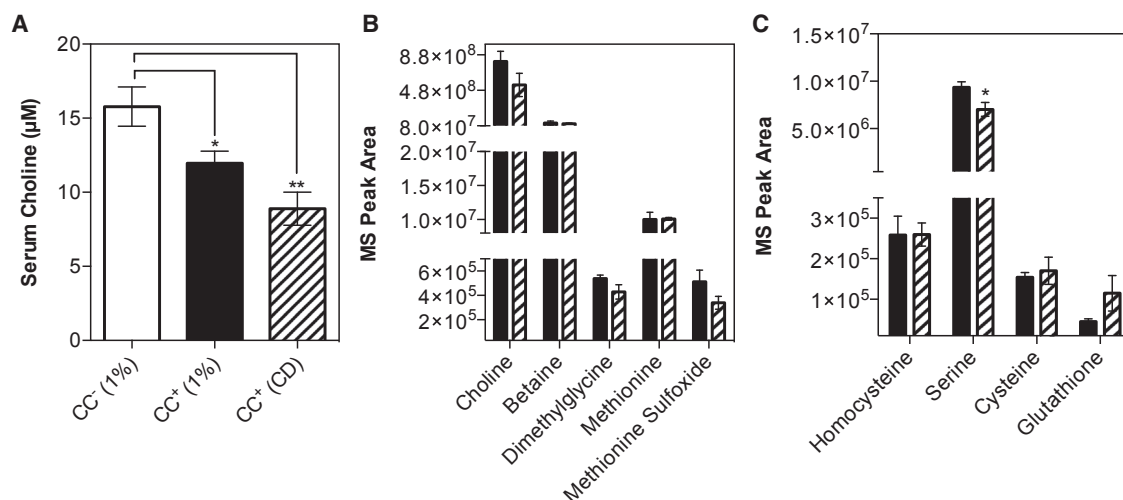


**Figure 4. Analysis of One-Carbon and Purine Metabolism in Serum from Mice Maintained on a Choline-Supplemented Diet versus Choline-Deficient Diet**

C57BL/6 females were colonized with the CC<sup>+</sup> community and maintained for 2 weeks on either a 1% (w/w) choline-supplemented diet or choline-deficient diet. Mice were fasted for 4 hr prior to sacrifice and serum collected. Serum metabolome analysis was conducted using uHPLC-MS/MS (five animals in each experimental group).

(A) Serum choline levels.

(B and C) Serum levels of metabolites involved in (B) one-carbon metabolism and (C) transsulfuration pathway.

All values are averages  $\pm$  SEMs. Values that were significantly different (Student's t test) are indicated: \* $p < 0.05$ ; \*\* $p < 0.01$ .

The molecular and biochemical signatures elicited by bacterial choline utilization are similar to those caused by choline deficiency. We further investigated how the serum levels of choline in CC<sup>+</sup> mice compared to those of CC<sup>+</sup> mice fed a choline-deficient diet (Envigo TD.88052). We found that choline levels in mice colonized with the CC<sup>+</sup> community maintained on a 1% choline diet did not differ significantly from those in mice colonized with the same community maintained on a choline-deficient diet. Both groups of mice showed significantly lower levels of choline compared to mice colonized with the CC<sup>-</sup> community fed a 1% choline diet (Figure 4A). Mice colonized with the CC<sup>+</sup> community maintained on a choline-supplemented versus a choline-deficient diet exhibited no differences in the abundance of metabolites involved in the generation of SAM (choline, betaine, methionine, dimethylglycine, and methionine sulfoxide) and most metabolites involved in the transsulfuration pathway (Figures 4B and 4C). However, the metabolomes from both treatment groups were not identical; for example, metabolites associated with purine metabolism (i.e., inosine, hypoxanthine, xanthine, kynurenine, and uric acid) were detected at lower levels in mice maintained on the choline-deficient diet compared to the CC<sup>+</sup> mice maintained on a 1% choline diet (Figure S2). Altogether, these results suggest that while gut microbial choline metabolism can impact nutrient bioavailability in ways that are consistent with dietary choline deficiency, the alterations to the global metabolome are not as stark as those imparted by a choline-depleted diet.

#### Bacterial Choline Metabolism Alters Global DNA Methylation and Exacerbates Diet-Induced Metabolic Disease

Many enzymes that impart epigenetic modifications, such as those that add and remove methyl groups to DNA and histones,

are highly sensitive to intracellular metabolite levels (Keating and El-Osta, 2015). Extended periods of dietary methyl-donor deficiency can not only alter epigenetic profiles but also promote the development of metabolic disease (Pogribny and Beland, 2009). Previous work suggests that chronic HF feeding exacerbates methyl-donor deficiencies (Craig, 2004). We tested the contribution of microbial choline metabolism to the development of diet-induced metabolic disease in mice sustained on an HF diet. Groups of mice colonized with the CC<sup>+</sup> and CC<sup>-</sup> community were maintained on an HF (42% Kcal) diet supplemented with 1% choline (Envigo TD.150782) for 8 weeks. Global DNA methylation assays revealed that mice colonized with the CC<sup>+</sup> community had lower levels of DNA methylation across multiple tissues (brain, heart, liver, and colon) relative to mice colonized with the CC<sup>-</sup> community (Figure 5A). Additionally, these mice showed significantly higher levels of TMAO (Figure 5B), inguinal fat accumulation (Figure 5D), and circulating leptin levels (Figure 5E), while having similar body weight (Figure 5C). Similar adiposity phenotypes as a result of microbial choline metabolism were observed 2 weeks after colonization on a 1% choline diet (normal fat) (Figure S3).

Enlargement of adipose tissue increases the release of free fatty acids (FFAs) into circulation and impairs FFA clearance (Björntorp et al., 1969). Circulating FFAs are taken up by the liver, where they are either oxidized to produce energy or re-esterified into triglycerides (TGs) (Boden et al., 2001). On an HF diet there is a large demand for phosphatidylcholine (PtdCho), which can be synthesized from free choline (Kennedy and Weiss, 1956). Hepatic PtdCho is required for assembly and secretion of VLDLs, and impairment of VLDL assembly/secretion contributes to the induction of hepatic steatosis (Fungwe et al., 1992). When PtdCho synthesis is impeded by reduced choline bioavailability, TG, a constituent of VLDLs, accumulates in the liver. Induction of

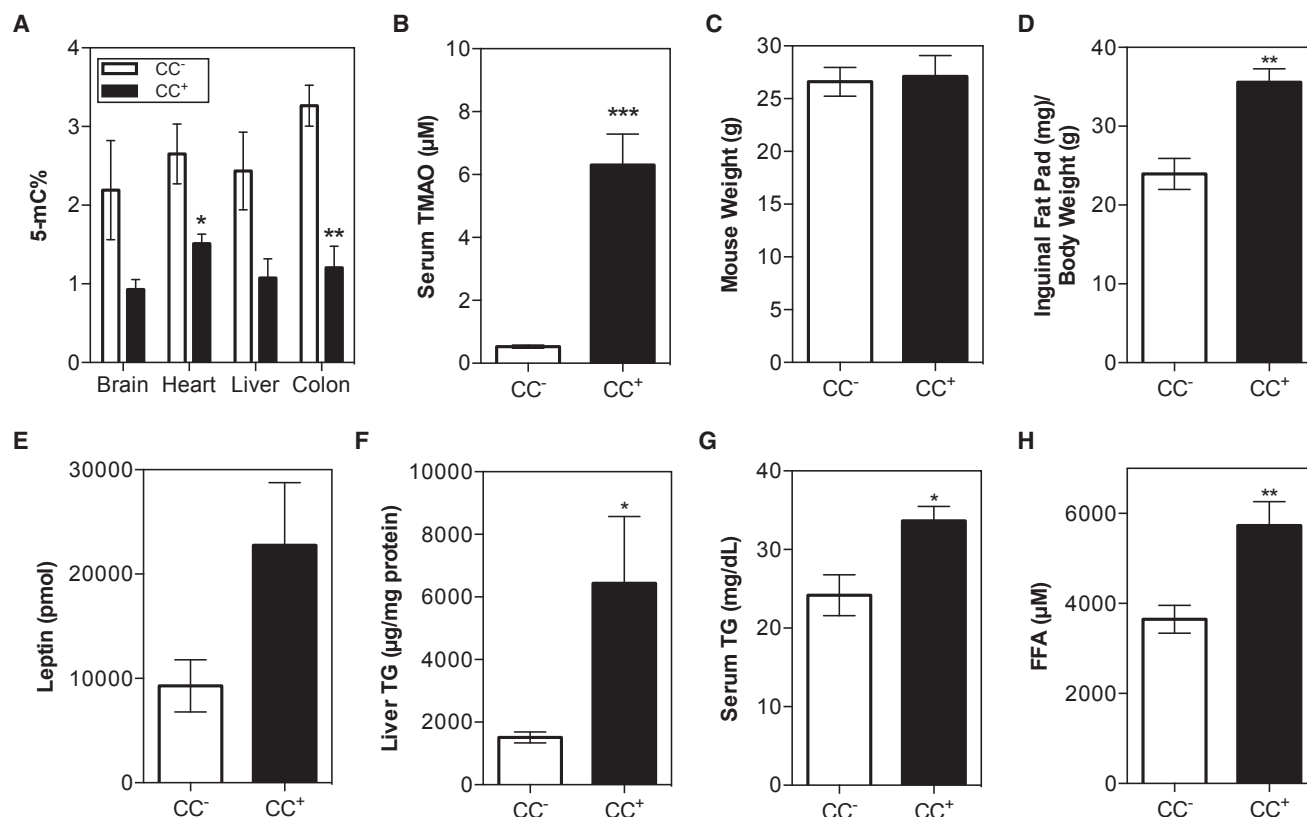


**Figure 5. Impact of Sustained Microbial Choline Consumption on Metabolic Disease and Global DNA Methylation Profiles**

C57BL/6 females (six animals in each experimental group) were colonized with either CC<sup>+</sup> or CC<sup>-</sup> community and maintained for 8 weeks on an HF (42% Kcal) + 1% (w/w) choline diet. Mice were fasted for 8 hr prior to sacrifice.

(A) Global DNA methylation. DNA was extracted and normalized as detailed in the STAR Methods. DNA methylation was determined using a colorimetric ELISA kit for brain, heart, liver, and colon.

(B) Serum TMAO.

(C) Mouse weight.

(D) Inguinal fat pad mass normalized to body weight.

(E) Leptin levels in serum.

(F) Hepatic TG levels normalized to protein concentration.

(G) Serum TG levels.

(H) Serum FFA levels.

All values are averages  $\pm$  SEMs. Values that were significantly different (Student's t test) are indicated: \* $p < 0.05$ , \*\* $p < 0.01$ , \*\*\* $p < 0.001$ .

hepatic steatosis also increases circulating TGs by a variety of mechanisms (Choi and Ginsberg, 2011). We found that hepatic and plasma TG levels (Figures 5F and 5G), as well as circulating FFA levels (Figure 5H), were elevated in the CC<sup>+</sup> group. While both TMAO accumulation and choline deficiency have been linked with NAFLD development, only TMAO has been previously associated with increases in visceral fat mass (Randrianarisoa et al., 2016). Altogether these results show that microbial choline utilization exacerbates metabolic disease, and the combined effects of limited choline availability and TMAO accumulation may synergize to promote adipogenesis (Figure S4).

### Maternal Gut Microbial Choline Metabolism Alters DNA Methylation in the Brains of Developing Neonates and Increases Anxiety

There is a high demand for choline during pregnancy. Choline is required during fetal development for regulating stem cell prolif-

eration, affects neural tube formation, and influences lifelong memory function (Zeisel, 2006). The results presented above show that microbial choline metabolism lowers choline and methyl donor bioavailability to the host. We assessed whether gut microbial choline utilization influences DNA methylation in mothers and offspring. Male and female GF C57BL/6 mice were colonized with either the CC<sup>-</sup> or CC<sup>+</sup> community described above and maintained on a 1% choline diet (normal fat content) for 4 weeks prior to the establishment of mating pairs. Pregnant mothers were sacrificed and pups collected by C-section when neonates were at the embryonic day 16 (E16)–E17.5 developmental stages (i.e., days post-fertilization, birth occurs at E18.5). TMAO (Figure 6A) was detected in plasma collected from mothers colonized with the CC<sup>+</sup> community and fetal tissue (liver) from their pups (Figure 6B). This finding is consistent with human data showing detectable levels of TMAO in the first urine passed by neonates (Foxall et al., 1995). Plasma levels of choline



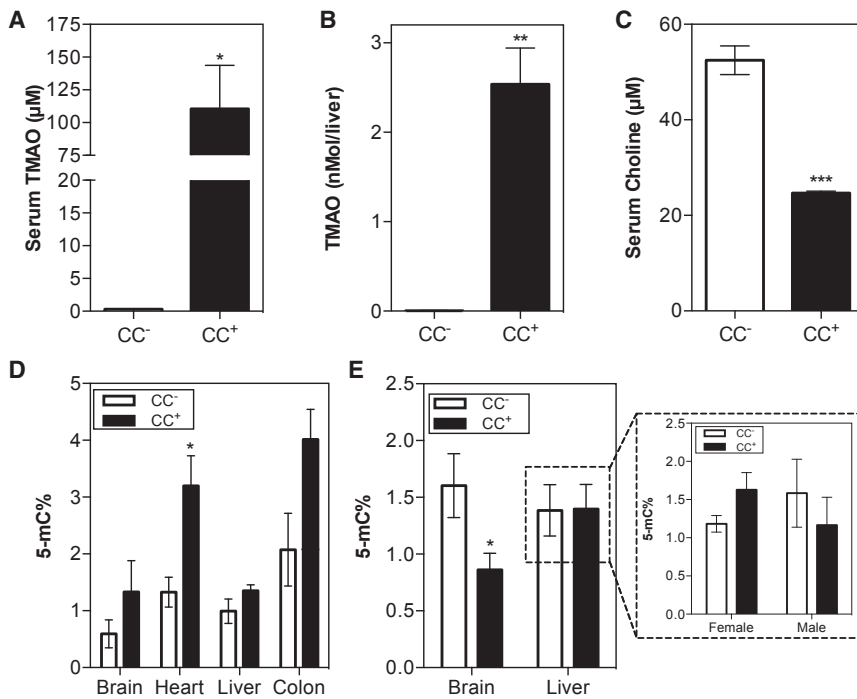


### Figure 6. Intergenerational Effects of Gut Microbial Choline Consumption

C57BL/6 males and females (three animals per sex) were colonized with either the CC<sup>+</sup> or CC<sup>-</sup> community and maintained for 4 weeks on a 1% (w/w) choline diet. Mating pairs were formed (three pairs per community) and females were monitored for vaginal plug formation. Females were sacrificed 17 days after visual confirmation of a vaginal plug/pregnancy and neonates were collected via C-section.

(A) Maternal serum TMAO levels.

(B) Fetal liver TMAO levels.

(C) Maternal serum choline levels.

(D) Global DNA methylation of mothers.

(E) Global DNA methylation of F<sub>1</sub> offspring. Neonates were sexed by PCR. DNA extracted from the brain and livers of ten neonates for each community (five female and five male). DNA methylation was determined using a colorimetric ELISA kit.

All values are averages ± SEMs. Values that were significantly different (Student's t test) are indicated: \*p < 0.05; \*\*\*p < 0.001.

(Figure 6C) and DNA methylation patterns (Figure 6D) in the mothers were comparable to non-pregnant females colonized with the same communities (Figures 2C and S3I). Interestingly, global DNA methylation patterns in both pregnant and non-pregnant females were increased in the CC<sup>+</sup> compared to CC<sup>-</sup> colonized animals. While this differs from the hypomethylation observed in the CC<sup>+</sup> colonized animals consuming HF+1% choline diet (Figure 5A), it is in line with previous reports in which female mice showed increased global methylation in response to methyl-donor deficiency (Nohara et al., 2011). These findings highlight the complex metabolic interactions that modulate epigenetic regulation, particularly the different methyl-donor demands imposed by different diets (HF versus low-fat diet). Additionally, we detected a significant reduction in DNA methylation levels in the brains, but not the livers, of neonates collected from CC<sup>+</sup> mothers (Figure 6E). However, DNA methylation patterns in the liver appear to be impacted differently as a function of sex (Figure 6E). This result is consistent with previous work showing sexual dimorphism in global DNA methylation profiles caused by methyl-donor deficiency (Nohara et al., 2011). Differences in global methylation patterns between tissues may reflect different demands for methyl donors during development. Altogether, these results show that choline utilization status of the intestinal microbiota in parents can affect maternal methyl donor availability and DNA methylation profiles as well as the offspring's epigenetic status in utero.

Previous studies have shown that offspring from mothers supplemented with choline during the latter half of pregnancy avoid any overt signs of age-associated cognitive decline (Zeisel and da Costa, 2009). Potential mechanisms for cognitive decline associated with suboptimal choline intake include reduced sphingomyelin abundance (a choline lipid derivative that is the main lipid in myelin sheaths) (Brody et al., 1987), reduced acetyl-

choline levels (Picciotto et al., 2012), and/or altered epigenetic regulation, including DNA methylation, which is known to play a pivotal role in complex brain functions (Wang et al., 2016). We tested whether changes in methyl donor levels in parents were associated with behavioral modifications in young adult animals that were both indirectly (in utero) and directly (after birth) exposed to gut microbial choline consumption. For these experiments, we used *Apoe*<sup>-/-</sup> mice because of their genetic predisposition for altered behavior. Specifically, APOE-deficient mice have cholinergic deficits that impair learning and memory as well as alter fear perception (Gordon et al., 1995). Previous studies showed that APOE-deficient mice were unable to learn new tasks, had impaired spatial memory/reasoning, and developed unusual repetitive behaviors (Oitzl et al., 1997).

Male and female GF *Apoe*<sup>-/-</sup> mice were colonized with either the CC<sup>-</sup> or CC<sup>+</sup> community and maintained on a 1% choline diet (normal fat content) for 4 weeks prior to the establishment of mating trios. Pregnancies were carried to term and pups were weaned 20 days after birth onto the same diet the parents were consuming. During nursing, parents colonized with the CC<sup>+</sup> community exhibited increased levels of infanticide (Figure 7A). F<sub>1</sub> offspring displayed circulating TMAO levels equivalent to colonized adults harboring the same communities (Figure 7B). Behavior (anxiety) was assessed in F<sub>1</sub> mice using a marble-burying assay at 8 weeks of age. Pups born to mothers colonized with the CC<sup>+</sup> community buried significantly more marbles than their CC<sup>-</sup> counterparts, regardless of sex (Figure 7C). Additionally, *Apoe*<sup>-/-</sup> mice (F<sub>0</sub>) colonized with the CC<sup>+</sup> community during adulthood displayed excessive barbering behaviors not observed in the CC<sup>-</sup> control group (Figure S5). Barbering is considered an abnormal repetitive behavior, and increased barbering has been observed in mouse models of anxiety and depressive-like behavior (Pereda et al., 2015). Altogether these results suggest

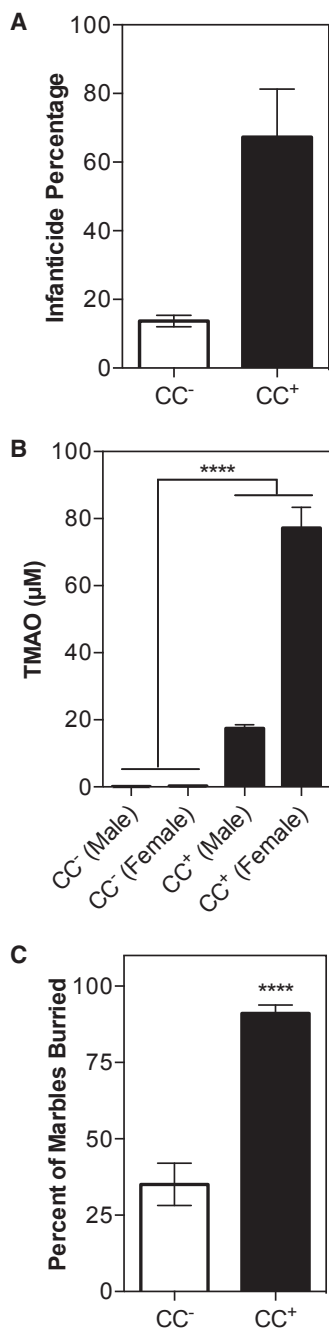


**Figure 7. Bacterially Induced Methyl-Donor Deficiency Increases Anxious Behaviors**

*Apoe*<sup>-/-</sup> males and females were colonized with either the CC<sup>+</sup> or CC<sup>-</sup> community and maintained for 4 weeks on a 1% (w/w) choline diet. Mating trios were formed (two per community) and mothers carried pregnancies to term.

(A) Parental infanticide. Pup survival was monitored during nursing. Bars represent average percentage of pups killed by infanticide over the course of two independent litters by four mothers/two fathers per community.

(B) F<sub>1</sub> serum TMAO levels. Community composition can be found in Figure S6. (C) Percentage of marbles buried by offspring (male and female) of GF *Apoe*<sup>-/-</sup> colonized with either the CC<sup>+</sup> or CC<sup>-</sup> community (n = 11–20/community).

All values are averages ± SEMs. Values that were significantly different (Student's t test) are indicated: \*\*\*\*p < 0.0001.

that methyl-donor depletion induced by gut microbes alters epigenetic regulation and behavior both in parents and offspring.

## DISCUSSION

This work links the presence of a single bacterial gene present in the human gut (*cutC*) with (1) changes in bacterial fitness, (2) the metabolic fate of the essential nutrient choline, (3) modifications in the host epigenome, and (4) susceptibility to metabolic disease and alterations in behavior. We show that harboring gut bacteria capable of transforming choline into TMA not only increases plasma levels of TMAO, but also decreases the bioavailability of choline and downstream metabolites involved in one-carbon metabolism. To date, the most definitive studies linking TMAO with the development of disease have used oral TMAO administration to mice as a method for increasing levels in circulation. However, TMAO production in vivo is linked to microbial consumption of specific substrates, including choline (Romano et al., 2015). Our results suggest that choline-consuming, TMA-producing gut microbes can significantly impact health not only through TMAO accumulation, but also by competing with the host for this essential nutrient, eliciting a quasi-choline-deficient state. This previously ignored aspect of microbial choline metabolism could have major implications for health and development, especially during pregnancy.

Epigenetic mechanisms provide a direct link between the environment (e.g., diet) and regulation of gene expression. While DNA methylation is in part regulated by non-modifiable genetic risk factors (e.g., SNPs in one-carbon metabolism enzymes), it is profoundly affected by modifiable dietary factors. Methylation reactions depend heavily on a steady input of methyl-donor precursors, including choline, folate, and betaine, which are obtained through our daily diet (Pogribny and Beland, 2009). We found that microbial choline utilization affected DNA methylation patterns across multiple tissues in adult mice while simultaneously increasing adiposity (Figures 5A, 5D, and S3). Previous studies have shown that disruption of epigenetic mechanisms significantly impacts the development of metabolic disease by increasing oxidative stress, reducing chromosome stability, and promoting the development of obesity, insulin resistance, and vascular dysfunction (Campión et al., 2009; Lavebratt et al., 2012; Martínez et al., 2014; Wang et al., 2012). Interestingly TMAO levels have also been positively associated with visceral fat mass (Randrianarisoa et al., 2016). Altogether, this suggests that microbial choline metabolism exacerbates diet-induced obesity by altering the host epigenome and gene expression.

We also explored the impact of gut microbial choline metabolism during pregnancy, a life period characterized by an exceptionally high demand for methyl donors. Maternal deficiency in dietary choline intake reduces global DNA methylation in the hippocampus in utero and impacts the development and function of cholinergic neurons that participate in learning, memory, and attention (Mellott et al., 2007; Zeisel, 2007). Consistent with these previous observations, our findings (Figure 6E) suggest that maternal gut microbial metabolism of choline alters its bioavailability in the developing fetus, which in turn affects the offspring's brain epigenome and behavior.

This study illustrates the value of using gnotobiotic mice colonized with engineered synthetic microbial communities for

dissecting the role(s) of individual gut microbial metabolic pathways. A potential drawback of this approach may be that effects of a single species, gene, or pathway may be overestimated due to an increased representation in a less competitive environment. Nonetheless, it should be noted that (1) high levels of choline-utilizing bacteria may not be required to efficiently compete with the host for choline (Romano et al., 2015); (2) single species often represent a large fraction of the human gut microbiome, particularly during dysbiosis (Qin et al., 2010); and (3) this last point is particularly relevant for species that can use molecules produced during inflammation (e.g., nitrate) to support choline consumption (Figure 1F) (Winter et al., 2013). Furthermore, human studies have revealed large interpersonal differences in the amount of TMAO generated from a uniform bolus of dietary choline, implying that some gut microbiomes convert choline to TMA more efficiently than others (Miller et al., 2014). Altogether, this evidence suggests that in addition to diet and host genetics, the gut microbiota is an important factor modulating choline bioavailability and that microbial metabolic capabilities should be examined on an individual basis when establishing nutritional requirements for optimal health and development.

## STAR★METHODS

Detailed methods are provided in the online version of this paper and include the following:

- KEY RESOURCES TABLE
- CONTACT FOR REAGENT AND RESOURCE SHARING
- EXPERIMENTAL MODEL AND SUBJECT DETAILS
  - Bacterial Strains and Growth Conditions
  - Construction of *Cut* Null Mutants
  - Gnotobiotic Studies
- METHOD DETAILS
  - Complementation Studies
  - Growth Studies
  - Quantitation of TMA Production from Choline
  - Community Profiling by Sequencing
  - qRT-PCR
  - RNaseq Library Prep
  - RNaseq Analysis
  - Serum and Hepatic Metabolite Extraction
  - uHPLC/MS/MS Metabolome Profiling
  - Marble-Burying Assay
  - Neonate sexing
  - Hepatic Triglyceride Quantification
  - Serum Triglyceride Quantification
  - DNA Global Methylation Assay
  - Free Fatty Acids Assay
  - Leptin Assay
  - Community Profiling by 16S rRNA Gene Sequencing
- QUANTIFICATION AND STATISTICAL ANALYSIS
- DATA AND SOFTWARE AVAILABILITY

## SUPPLEMENTAL INFORMATION

Supplemental Information includes six figures and two tables and can be found with this article online at <http://dx.doi.org/10.1016/j.chom.2017.07.021>.

## AUTHOR CONTRIBUTIONS

Conceptualization, K.A.R., A.M.-d.C., E.P.B., and F.E.R.; Methodology, K.A.R., A.M.-d.C., K.K., E.I.V., D.A.-N., E.P.B., and F.E.R.; Formal Analysis, K.A.R. and A.M.-d.C.; Investigation, K.A.R., A.M.-d.C., K.K., and C.L.C.; Resources, A.M.-d.C., C.L.C., E.I.V., and D.A.-N.; Data Curation, K.A.R.; Writing – Original Draft, K.A.R., A.M.-d.C., E.P.B., and F.E.R.; Writing – Review & Editing, K.A.R., A.M.-d.C., K.K., C.L.C., E.I.V., D.A.-N., E.P.B., and F.E.R.; Visualization, K.A.R., A.M.-d.C., K.K., and C.L.C.; Supervision, D.A.-N., E.P.B., and F.E.R.; Funding Acquisition, D.A.-N., E.P.B., and F.E.R.

## ACKNOWLEDGMENTS

The authors thank the University of Wisconsin Biotechnology Center DNA Sequencing Facility for providing sequencing and support services and the University of Wisconsin Center for High Throughput Computing (CHTC) in the Department of Computer Sciences for providing computational resources, support, and assistance. Our deepest gratitude to Kimberly Dill-McFarland and Leticia Reyes for experimental assistance in response to reviewer comments. We also thank David Stevenson for technical support, Danish A. Khan and Kimberly A. Krautkramer for assistance with bioinformatic analyses, Robert Kerby for helpful comments during the course of these studies, and Fredrik Bäckhed for supplying germ-free *Apoe*<sup>-/-</sup> mice. The project described was supported in part by NIH DK108259 (F.E.R.), a Smith Family Award for Biomedical Research (E.P.B.), a Packard Fellowship for Science and Engineering (2013-39267) (E.P.B.), and a Blavatnik Biomedical Accelerator Award (E.P.B.). This material is based upon work that is supported by the National Institute of Food and Agriculture, U.S. Department of Agriculture WIS01910, and Hatch WIS01901.

Received: January 31, 2017

Revised: June 13, 2017

Accepted: July 31, 2017

Published: August 24, 2017

## SUPPORTING CITATIONS

The following references appear in the Supplemental Information: Ahima and Flier (2000); Huang et al. (2006); Pekkala et al. (2015); Siersbaek et al. (2010); Wang et al. (1999).

## REFERENCES

- Ahima, R.S., and Flier, J.S. (2000). Adipose tissue as an endocrine organ. *Trends Endocrinol. Metab.* *11*, 327–332.
- Baker, J.R., and Chaykin, S. (1962). The biosynthesis of trimethylamine-N-oxide. *J. Biol. Chem.* *237*, 1309–1313.
- Bay, D.C., and Turner, R.J. (2012). Small multidrug resistance protein EmrE reduces host pH and osmotic tolerance to metabolic quaternary cation osmoprotectants. *J. Bacteriol.* *194*, 5941–5948.
- Bhandary, B., Marahatta, A., Kim, H.-R., and Chae, H.-J. (2012). An involvement of oxidative stress in endoplasmic reticulum stress and its associated diseases. *Int. J. Mol. Sci.* *14*, 434–456.
- Björntorp, P., Bergman, H., and Varnauskas, E. (1969). Plasma free fatty acid turnover rate in obesity. *Acta Med. Scand.* *185*, 351–356.
- Bligh, E.G., and Dyer, W.J. (1959). A rapid method of total lipid extraction and purification. *Can. J. Biochem. Physiol.* *37*, 911–917.
- Boden, G., Lebed, B., Schatz, M., Homko, C., and Lemieux, S. (2001). Effects of acute changes of plasma free fatty acids on intramyocellular fat content and insulin resistance in healthy subjects. *Diabetes* *50*, 1612–1617.
- Brody, B.A., Kinney, H.C., Kloman, A.S., and Gilles, F.H. (1987). Sequence of central nervous system myelination in human infancy. I. An autopsy study of myelination. *J. Neuropathol. Exp. Neurol.* *46*, 283–301.
- Brunst, K.J., Wright, R.O., DiGioia, K., Enlow, M.B., Fernandez, H., Wright, R.J., and Kannan, S. (2014). Racial/ethnic and sociodemographic factors

- associated with micronutrient intakes and inadequacies among pregnant women in an urban US population. *Public Health Nutr.* 17, 1960–1970.
- Campión, J., Milagro, F.I., and Martínez, J.A. (2009). Individuality and epigenetics in obesity. *Obes. Rev.* 10, 383–392.
- Chen, Y., Jameson, E., Doxey, A.C., Airs, R., Purdy, K.J., and Murrell, J.C. (2016). Metagenomic data-mining reveals contrasting microbial populations responsible for trimethylamine formation in human gut and marine ecosystems. *Microb. Genomics* 2, <http://dx.doi.org/10.1099/mgen.0.000080>.
- Choi, S.H., and Ginsberg, H.N. (2011). Increased very low density lipoprotein (VLDL) secretion, hepatic steatosis, and insulin resistance. *Trends Endocrinol. Metab.* 22, 353–363.
- Craciun, S., and Balskus, E.P. (2012). Microbial conversion of choline to trimethylamine requires a glycol radical enzyme. *Proc. Natl. Acad. Sci. USA* 109, 21307–21312.
- Craig, S.A.S. (2004). Betaine in human nutrition. *Am. J. Clin. Nutr.* 80, 539–549.
- Dambrova, M., Latkovskis, G., Kuka, J., Strele, I., Konrade, I., Grinberga, S., Hartmane, D., Pugovics, O., Erglis, A., and Liepinsh, E. (2016). Diabetes is associated with higher trimethylamine N-oxide plasma levels. *Exp. Clin. Endocrinol. Diabetes* 124, 251–256.
- Datsenko, K.A., and Wanner, B.L. (2000). One-step inactivation of chromosomal genes in *Escherichia coli* K-12 using PCR products. *Proc. Natl. Acad. Sci. USA* 97, 6640–6645.
- Deminice, R., de Castro, G.S.F., Francisco, L.V., da Silva, L.E.C.M., Cardoso, J.F.R., Frajacomo, F.T.T., Teodoro, B.G., Dos Reis Silveira, L., and Jordao, A.A. (2015). Creatine supplementation prevents fatty liver in rats fed choline-deficient diet: a burden of one-carbon and fatty acid metabolism. *J. Nutr. Biochem.* 26, 391–397.
- Dykxhoorn, D.M., St Pierre, R., and Linn, T. (1996). A set of compatible tac promoter expression vectors. *Gene* 177, 133–136.
- Falony, G., Vieira-Silva, S., and Raes, J. (2015). Microbiology meets big data: the case of gut microbiota-derived trimethylamine. *Annu. Rev. Microbiol.* 69, 305–321.
- Foxall, P.J., Bewley, S., Neild, G.H., Rodeck, C.H., and Nicholson, J.K. (1995). Analysis of fetal and neonatal urine using proton nuclear magnetic resonance spectroscopy. *Arch. Dis. Child. Fetal Neonatal* 73, F153–F157.
- Fungwe, T.V., Cagen, L., Wilcox, H.G., and Heimberg, M. (1992). Regulation of hepatic secretion of very low density lipoprotein by dietary cholesterol. *J. Lipid Res.* 33, 179–191.
- Gordon, I., Grauer, E., Genis, I., Sehayek, E., and Michaelson, D.M. (1995). Memory deficits and cholinergic impairments in apolipoprotein E-deficient mice. *Neurosci. Lett.* 199, 1–4.
- Huang, W., Dedouis, N., Bandi, A., Lopaschuk, G.D., and O'Doherty, R.M. (2006). Liver triglyceride secretion and lipid oxidative metabolism are rapidly altered by leptin in vivo. *Endocrinology* 147, 1480–1487.
- Keating, S.T., and El-Osta, A. (2015). Epigenetics and metabolism. *Circ. Res.* 116, 715–736.
- Kennedy, E.P., and Weiss, S.B. (1956). The function of cytidine coenzymes in the biosynthesis of phospholipides. *J. Biol. Chem.* 222, 193–214.
- Koeth, R.A., Wang, Z., Levison, B.S., Buffa, J.A., Org, E., Sheehy, B.T., Britt, E.B., Fu, X., Wu, Y., Li, L., et al. (2013). Intestinal microbiota metabolism of L-carnitine, a nutrient in red meat, promotes atherosclerosis. *Nat. Med.* 19, 576–585.
- Kozich, J.J., Westcott, S.L., Baxter, N.T., Highlander, S.K., and Schloss, P.D. (2013). Development of a dual-index sequencing strategy and curation pipeline for analyzing amplicon sequence data on the MiSeq Illumina sequencing platform. *Appl. Environ. Microbiol.* 79, 5112–5120.
- Lamark, T., Røkenes, T.P., McDougall, J., and Strøm, A.R. (1996). The complex bet promoters of *Escherichia coli*: regulation by oxygen (ArcA), choline (BetI), and osmotic stress. *J. Bacteriol.* 178, 1655–1662.
- Langmead, B., and Salzberg, S.L. (2012). Fast gapped-read alignment with Bowtie 2. *Nat. Methods* 9, 357–359.
- Lavebratt, C., Almgren, M., and Ekström, T.J. (2012). Epigenetic regulation in obesity. *Int. J. Obes.* 36, 757–765.
- Leng, N., Dawson, J.A., Thomson, J.A., Ruotti, V., Rissman, A.I., Smits, B.M.G., Haag, J.D., Gould, M.N., Stewart, R.M., and Kendziorzi, C. (2013). EBSeq: an empirical Bayes hierarchical model for inference in RNA-seq experiments. *Bioinformatics* 29, 1035–1043.
- Li, B., and Dewey, C.N. (2011). RSEM: accurate transcript quantification from RNA-seq data with or without a reference genome. *BMC Bioinformatics* 12, 323.
- Martínez, J.A., Milagro, F.I., Claycombe, K.J., and Schalinske, K.L. (2014). Epigenetics in adipose tissue, obesity, weight loss, and diabetes. *Adv. Nutr.* 5, 71–81.
- Martínez-del Campo, A., Bodea, S., Hamer, H.A., Marks, J.A., Haiser, H.J., Turnbaugh, P.J., and Balskus, E.P. (2015). Characterization and detection of a widely distributed gene cluster that predicts anaerobic choline utilization by human gut bacteria. *MBio* 6, e00042–15.
- McFarlane, L., Truong, V., Palmer, J.S., and Wilhelm, D. (2013). Novel PCR assay for determining the genetic sex of mice. *Sex Dev.* 7, 207–211.
- McMahon, K.E., and Farrell, P.M. (1985). Measurement of free choline concentrations in maternal and neonatal blood by micropyrolysis gas chromatography. *Clin. Chim. Acta* 149, 1–12.
- McNulty, N.P., Yatsunenko, T., Hsiao, A., Faith, J.J., Muegge, B.D., Goodman, A.L., Henrissat, B., Oozeer, R., Cools-Portier, S., Gobert, G., et al. (2011). The impact of a consortium of fermented milk strains on the gut microbiome of gnotobiotic mice and monozygotic twins. *Sci. Transl. Med.* 3, 106ra106.
- Melamud, E., Vastag, L., and Rabinowitz, J.D. (2010). Metabolomic analysis and visualization engine for LC-MS data. *Anal. Chem.* 82, 9818–9826.
- Mellott, T.J., Kowall, N.W., Lopez-Coviella, I., and Blusztajn, J.K. (2007). Prenatal choline deficiency increases choline transporter expression in the septum and hippocampus during postnatal development and in adulthood in rats. *Brain Res.* 1151, 1–11.
- Miller, C.A., Corbin, K.D., da Costa, K.-A., Zhang, S., Zhao, X., Galanko, J.A., Blevins, T., Bennett, B.J., O'Connor, A., and Zeisel, S.H. (2014). Effect of egg ingestion on trimethylamine-N-oxide production in humans: a randomized, controlled, dose-response study. *Am. J. Clin. Nutr.* 100, 778–786.
- Mudd, S.H., and Poole, J.R. (1975). Labile methyl balances for normal humans on various dietary regimens. *Metabolism* 24, 721–735.
- Nohara, K., Baba, T., Murai, H., Kobayashi, Y., Suzuki, T., Tateishi, Y., Matsumoto, M., Nishimura, N., and Sano, T. (2011). Global DNA methylation in the mouse liver is affected by methyl deficiency and arsenic in a sex-dependent manner. *Arch. Toxicol.* 85, 653–661.
- Oitzl, M.S., Mulder, M., Lucassen, P.J., Havekes, L.M., Grootendorst, J., and de Kloet, E.R. (1997). Severe learning deficits in apolipoprotein E-knockout mice in a water maze task. *Brain Res.* 752, 189–196.
- Ozarda Ilcol, Y., Uncu, G., and Ulus, I.H. (2002). Free and phospholipid-bound choline concentrations in serum during pregnancy, after delivery and in newborns. *Arch. Physiol. Biochem.* 110, 393–399.
- Pekkala, S., Munukka, E., Kong, L., Pöllänen, E., Autio, R., Roos, C., Wiklund, P., Fischer-Posovszky, P., Wabitsch, M., Alen, M., et al. (2015). Toll-like receptor 5 in obesity: the role of gut microbiota and adipose tissue inflammation. *Obesity (Silver Spring)* 23, 581–590.
- Pereda, D., Pardo, M.R., Morales, Y., Dominguez, N., Arnau, M.R., and Borges, R. (2015). Mice lacking chromogranins exhibit increased aggressive and depression-like behaviour. *Behav. Brain Res.* 278, 98–106.
- Piccio, M.R., Higley, M.J., and Mineur, Y.S. (2012). Acetylcholine as a neuromodulator: cholinergic signaling shapes nervous system function and behavior. *Neuron* 76, 116–129.
- Pisithkul, T., Jacobson, T.B., O'Brien, T.J., Stevenson, D.M., and Amador-Noguez, D. (2015). Phenolic amides are potent inhibitors of *de novo* nucleotide biosynthesis. *Appl. Environ. Microbiol.* 81, 5761–5772.
- Pogribny, I.P., and Beland, F.A. (2009). DNA hypomethylation in the origin and pathogenesis of human diseases. *Cell. Mol. Life Sci.* 66, 2249–2261.
- Price-Carter, M., Tingey, J., Bobik, T.A., and Roth, J.R. (2001). The alternative electron acceptor tetrathionate supports B12-dependent anaerobic growth of *Salmonella enterica* serovar typhimurium on ethanolamine or 1,2-propanediol. *J. Bacteriol.* 183, 2463–2475.

- Qin, J., Li, R., Raes, J., Arumugam, M., Burgdorf, K.S., Manichanh, C., Nielsen, T., Pons, N., Levenez, F., Yamada, T., et al.; MetaHIT Consortium (2010). A human gut microbial gene catalogue established by metagenomic sequencing. *Nature* **464**, 59–65.
- Randrianarisoa, E., Lehn-Stefan, A., Wang, X., Hoene, M., Peter, A., Heinzmann, S.S., Zhao, X., Königsrainer, I., Königsrainer, A., Balletshofer, B., et al. (2016). Relationship of serum trimethylamine N-oxide (TMAO) levels with early atherosclerosis in humans. *Sci. Rep.* **6**, 26745.
- Romano, K.A., Vivas, E.I., Amador-Nogues, D., and Rey, F.E. (2015). Intestinal microbiota composition modulates choline bioavailability from diet and accumulation of the proatherogenic metabolite trimethylamine-N-oxide. *MBio* **6**, e02481.
- Ross, R.G., Hunter, S.K., Hoffman, M.C., McCarthy, L., Chambers, B.M., Law, A.J., Leonard, S., Zerbe, G.O., and Freedman, R. (2016). Perinatal phosphatidylcholine supplementation and early childhood behavior problems: evidence for *CHRNA7* moderation. *Am. J. Psychiatry* **173**, 509–516.
- Schloss, P.D., Westcott, S.L., Ryabin, T., Hall, J.R., Hartmann, M., Hollister, E.B., Lesniewski, R.A., Oakley, B.B., Parks, D.H., Robinson, C.J., et al. (2009). Introducing mothur: open-source, platform-independent, community-supported software for describing and comparing microbial communities. *Appl. Environ. Microbiol.* **75**, 7537–7541.
- Semba, R.D., Zhang, P., Gonzalez-Freire, M., Moaddel, R., Trehan, I., Maleta, K.M., Ordiz, M.I., Ferrucci, L., and Manary, M.J. (2016). The association of serum choline with linear growth failure in young children from rural Malawi. *Am. J. Clin. Nutr.* **104**, 191–197.
- Siersbaek, R., Nielsen, R., and Mandrup, S. (2010). PPARgamma in adipocyte differentiation and metabolism—novel insights from genome-wide studies. *FEBS Lett.* **584**, 3242–3249.
- Tang, W.H., Wang, Z., Kennedy, D.J., Wu, Y., Buffa, J.A., Agatista-Boyle, B., Li, X.S., Levison, B.S., and Hazen, S.L. (2015). Gut microbiota-dependent trimethylamine N-oxide (TMAO) pathway contributes to both development of renal insufficiency and mortality risk in chronic kidney disease. *Circ. Res.* **116**, 448–455.
- Turnbaugh, P.J., Hamady, M., Yatsunenkov, T., Cantarel, B.L., Duncan, A., Ley, R.E., Sogin, M.L., Jones, W.J., Roe, B.A., Affourtit, J.P., et al. (2009). A core gut microbiome in obese and lean twins. *Nature* **457**, 480–484.
- Vogel, H.J., and Bonner, D.M. (1956). Acetylornithinase of *Escherichia coli*: partial purification and some properties. *J. Biol. Chem.* **218**, 97–106.
- Wang, Z., and Storm, D.R. (2006). Extraction of DNA from mouse tails. *Biotechniques* **41**, 410, 412.
- Wang, J., Liu, R., Liu, L., Chowdhury, R., Barzilai, N., Tan, J., and Rossetti, L. (1999). The effect of leptin on *Lep* expression is tissue-specific and nutritionally regulated. *Nat. Med.* **5**, 895–899.
- Wang, Z., Klipfell, E., Bennett, B.J., Koeth, R., Levison, B.S., Dugar, B., Feldstein, A.E., Britt, E.B., Fu, X., Chung, Y.-M., et al. (2011). Gut flora metabolism of phosphatidylcholine promotes cardiovascular disease. *Nature* **472**, 57–63.
- Wang, J., Wu, Z., Li, D., Li, N., Dindot, S.V., Satterfield, M.C., Bazer, F.W., and Wu, G. (2012). Nutrition, epigenetics, and metabolic syndrome. *Antioxid. Redox Signal.* **17**, 282–301.
- Wang, Y., Surzenko, N., Friday, W.B., and Zeisel, S.H. (2016). Maternal dietary intake of choline in mice regulates development of the cerebral cortex in the offspring. *FASEB J.* **30**, 1566–1578.
- Westcott, S.L., and Schloss, P.D. (2017). OptiClust, an improved method for assigning amplicon-based sequence data to operational taxonomic units. *mSphere* **2**, e00073–17.
- Winter, S.E., Winter, M.G., Xavier, M.N., Thiennimitr, P., Poon, V., Keestra, A.M., Laughlin, R.C., Gomez, G., Wu, J., Lawhon, S.D., et al. (2013). Host-derived nitrate boosts growth of *E. coli* in the inflamed gut. *Science* **339**, 708–711.
- Zeisel, S.H. (2006). Choline: critical role during fetal development and dietary requirements in adults. *Annu. Rev. Nutr.* **26**, 229–250.
- Zeisel, S.H. (2007). Gene response elements, genetic polymorphisms and epigenetics influence the human dietary requirement for choline. *IUBMB Life* **59**, 380–387.
- Zeisel, S.H. (2012). Dietary choline deficiency causes DNA strand breaks and alters epigenetic marks on DNA and histones. *Mutat. Res.* **733**, 34–38.
- Zeisel, S.H., and da Costa, K.-A. (2009). Choline: an essential nutrient for public health. *Nutr. Rev.* **67**, 615–623.

## STAR★METHODS

## KEY RESOURCES TABLE

REAGENT or RESOURCE	SOURCE	IDENTIFIER
<b>Bacterial and Virus Strains</b>		
<i>Bacteroides caccae</i>	ATCC	43185
<i>Bacteroides ovatus</i>	ATCC	8483
<i>Bacteroides thetaiotaomicron</i> VPI-5482	ATCC	29148
<i>Collinsella aerofaciens</i>	ATCC	25986
<i>Eubacterium rectale</i>	ATCC	33656
<i>Escherichia coli</i>	BEI	MS 200-1
EMC	This study	MS 200-1 derivative, $\Delta cutC$
EMD	This study	MS 200-1 derivative, $\Delta cutD$
<b>Chemicals, Peptides, and Recombinant Proteins</b>		
Triton X	Sigma	Cat. # T8787-50ML
Trizol	Ambion	Cat. # 15596026
RNase Zap	Thermo Scientific	Cat. # AM9780
D9-Choline	Cambridge Isotope Laboratories	Cat. # DLM-549-1
D9-TMAO	Cambridge Isotope Laboratories	Cat. # DLM-4779-PK
Phenol:Chloroform:Isoamyl Alcohol (pH 7.9, 25:24:1)	Invitrogen	Cat. # 15593-049
HotStart ReadyMix	KAPA Biosystems	Cat. # 07958935001; Also known as KK2602
SYBR Green Supermix	BioRad	Cat. # 172-5271
T4 DNA Ligase	NEB	Cat. # M0202M
T4 Polymerase	NEB	Cat. # M0203L
T4 PNK	NEB	Cat. # M0201L
Taq Polymerase	Invitrogen	Cat. # 18038-042
GoTaq Green Master Mix (2X)	Promega	Cat. # M712B
SYBR Safe DNA Gel Stain	Invitrogen	Cat. # S33102
DpnI	NEB	Cat. # R0176S
<b>Critical Commercial Assays</b>		
Leptin (mouse) ELISA Kit	Enzo	Cat. # ADI-900-019A
Free Fatty Acid Assay Kit (Colorimetric)	Cell Biolabs	Cat. # STA-618
Illumina TruSeq stranded mRNA Sample Preparation Kit	Illumina	Cat. # RS-122-2101
MethylFlash Global DNA Methylation ELISA Easy Kit	EpiGentek	Cat. # P-1030-48; Cat. # P-1030-96
L-type Triglyceride M Kit	Wako Diagnostics	Cat. # 461-08992; Cat. # 461-09092; Cat. # 464-01601
NucleoSpin Gel and PCR Clean-up Kit	Macherey-Nagel	Cat. # 740609.250
ZR-96 ZymoClean Gel DNA Recovery Kit	Zymo Reserach	Cat. # D4021
RNeasy Mini Kit	QIAGEN	Cat. # 74104
Bradford Protein Assay Kit	BioRad	Cat. # 500-0201
<b>Deposited Data</b>		
RNaseq raw and processed reads	GEO	GEO: GSE100983
COPROseq and 16S rRNA gene raw reads	SRA	SRA: PRJNA393700
<b>Experimental Models: Organisms/Strains</b>		
<i>Mus musculus</i> C57BL/6	Germ-free mice raised in the gnotobiotic facility at the University of Wisconsin - Madison	N/A
<i>Mus musculus</i> C57BL/6 Apoe <sup>-/-</sup>	Germ-free mice raised in the gnotobiotic facility at the University of Wisconsin - Madison	N/A

(Continued on next page)

**Continued**

REAGENT or RESOURCE	SOURCE	IDENTIFIER
Oligonucleotides		
Oligonucleotides can be found in <a href="#">Table S2</a>	N/A	N/A
Recombinant DNA		
pKD119	CGSC	CGSC#: 7990
pKD3	CGSC	CGSC#: 7631
pEXT22	CGSC	CGSC#: 12327
pcutC (pEXT22 derivative carrying <i>cutC</i> )	This study	N/A
pcutD (pEXT22 derivative carrying <i>cutD</i> )	This study	N/A
Software and Algorithms		
GraphPad Prism	GraphPad Software	<a href="https://www.graphpad.com/scientific-software/prism/">https://www.graphpad.com/scientific-software/prism/</a>
EBSeq	<a href="#">Leng et al., 2013</a>	<a href="https://www.biostat.wisc.edu/~kendzior/EBSEQ/">https://www.biostat.wisc.edu/~kendzior/EBSEQ/</a>
RSEM	<a href="#">Li and Dewey, 2011</a>	<a href="https://deweylab.github.io/RSEM/">https://deweylab.github.io/RSEM/</a>
COPROseq	This study	<a href="https://github.com/DanishKhan14/aligner_RL">https://github.com/DanishKhan14/aligner_RL</a>
FASTX Toolkit	Hannon Lab	<a href="http://hannonlab.cshl.edu/fastx_toolkit/">http://hannonlab.cshl.edu/fastx_toolkit/</a>
Bowtie2	<a href="#">Langmead and Salzberg, 2012</a>	<a href="http://bowtie-bio.sourceforge.net/bowtie2/index.shtml">http://bowtie-bio.sourceforge.net/bowtie2/index.shtml</a>
Mouthr	<a href="#">Schloss et al., 2009</a>	<a href="https://www.mothur.org/">https://www.mothur.org/</a>
MAVEN	<a href="#">Melamud et al., 2010</a>	<a href="http://genomics-pubs.princeton.edu/mzroll/index.php">http://genomics-pubs.princeton.edu/mzroll/index.php</a>
Other		
1% Choline Diet	Envigo (Madison, WI)	TD.140179
Choline Deficient Diet	Envigo (Madison, WI)	TD.88052
High Fat (42% Kcal)+1% Choline Diet	Envigo (Madison, WI)	TD.150782
Bio-Bond C4 3 $\mu\text{m}$ 150 $\times$ 2.1 mm	Dikma	Cat. # 84413
ACQUITY UPLC BEH C18 Column, 130 $\text{\AA}$ , 1.7 $\mu\text{m}$ , 2.1 mm X 100 mm	Waters	Cat. # 186002352
Kinetex HILIC column (2.6 $\mu\text{m}$ , 30 mm $\times$ 2.1 mm, 100 $\text{\AA}$ )	Phenomenex	Cat. # 00A-4461-AN

**CONTACT FOR REAGENT AND RESOURCE SHARING**

Further information and requests for resources and reagents should be directed to and will be fulfilled by the Lead Contact, Federico Rey ([ferey@wisce.edu](mailto:ferey@wisce.edu)).

**EXPERIMENTAL MODEL AND SUBJECT DETAILS****Bacterial Strains and Growth Conditions**

All strains and plasmids used in this study are listed in the [Key Resources Table](#). *E. coli* strains and derivatives were grown on LB, BHI or no-carbon-E (NCE) medium ([Vogel and Bonner, 1956](#)). When needed, antibiotics were added to the media at the following concentrations: ampicillin (100  $\mu\text{g}/\text{ml}$ ), chloramphenicol (25  $\mu\text{g}/\text{ml}$ ), kanamycin (50  $\mu\text{g}/\text{ml}$ ), or tetracycline (25  $\mu\text{g}/\text{ml}$ ).

**Construction of *Cut* Null Mutants**

Non-polar deletion strains of *cutC* and *cutD* were generated using the lambda Red recombinase system ([Datsenko and Wanner, 2000](#)). Genes were replaced with a chloramphenicol resistance marker. PCR products were amplified using the template plasmid pKD3 and primers listed in the [Table S2](#). Following amplification products were digested with *DpnI* and gel-purified. Electrocompetent cells of *E. coli* MS 200-1 carrying the Red recombinase expression plasmid pKD119 (see the [Key Resources Table](#)) were transformed with the desired PCR product. After transformation, chloramphenicol-resistant and tetracycline-sensitive recombinants were selected at 37°C. Gene disruptions were confirmed by PCR using primers flanking the targeted region.

### Gnotobiotic Studies

All experiments involving mice were performed using protocols approved by the University of Wisconsin-Madison Animal Care and Use Committee. Strains used to colonize mice were grown as monocultures on Mega Medium agar plates anaerobically for 48 to 72 hr at 37°C. Single colonies were then inoculated into 3 mL of Mega Medium and grown anaerobically for 24 hr at 37°C. After 24 hr, strains belonging to the same treatment group were combined in an equal volume ratio in a Hungate tube. C57BL/6 germ-free mice (WT and *ApoE*<sup>-/-</sup>) were inoculated by oral gavage with ~0.2 mL of mixed bacterial culture inside the gnotobiotic isolator (Romano et al., 2015). Mice were maintained on the experimental diets (see Key Resources Table) for two weeks after colonization unless otherwise noted. Unless noted all experiments were performed in female mice. Animals used in acute experiments were colonized at 7 weeks of age and euthanized at 9 weeks of age, while those used in sustained experiments were colonized at 6 weeks of age and euthanized at 14 weeks of age. Mating pairs were colonized around 6 weeks of age and housed by sex for 4 weeks on a 1% choline diet prior to mating. Male and female F<sub>1</sub> pups collected by C-section (from ~14-week-old females) were sacrificed at E16-17.5. F<sub>1</sub> animals (females and males) used in behavior assays were 8 weeks of age. Prior to sacrifice mice were fasted for 4 hr in the regular diet and 8 hr in the High Fat+1% choline diet, unless noted. Mice were anesthetized with 1%–5% inhalant isoflurane supplied in oxygen. Tissue was immediately collected, flash frozen, and stored at –80°C.

### METHOD DETAILS

#### Complementation Studies

The *cutC* and *cutD* genes were PCR amplified using genomic DNA from strain *E. coli* MS 200-1 as the template (primers listed Table S2). The resulting products were cloned into the *EcoRI* and *XbaI* sites of the pEXT22 vector (Dykxhoom et al., 1996). Plasmids were transformed into the respective mutants by electroporation. The growth of these strains was assessed using the same conditions detailed in “Growth studies,” but adding 1 μM of IPTG to the medium to induce gene expression.

#### Growth Studies

To evaluate the phenotype of the wild-type *E. coli* MS 200-1 and the *cutC* and *cutD* null mutants, strains were grown in anoxic NCE medium supplemented with 15 mM choline, 40 mM fumarate, 1 mM MgSO<sub>4</sub>, 0.1% casaminoacids, 0.5 mM glucose, and 1% vitamin and trace mineral solutions (American Type Culture Collection). To evaluate the growth using different electron acceptors 40 mM nitrate, DMSO, TMAO, or tetrathionate were added instead of fumarate, and glucose was omitted from the media. Medium was sparged with N<sub>2</sub> and was dispensed inside an anaerobic chamber (atmosphere of 95% nitrogen and 5% hydrogen) into Hungate tubes. Tubes containing 5 mL of medium were inoculated with 50 μL of an overnight culture and incubated at 37°C for 48 hr. Growth was monitored as the increase in the absorbance at 600 nm in a Genesys 20 spectrophotometer (Thermo Fisher Scientific).

#### Quantitation of TMA Production from Choline

Strains were grown anaerobically on NCE plus fumarate medium containing 15 mM (trimethyl-d<sub>9</sub>)-choline (Cambridge Isotope Laboratories, Tewksbury, MA), 1 μM of IPTG and 0.5 mM glucose in order to quantify TMA produced by the wild-type and the *cutC* and *cutD* knock-out strains under these conditions. Three 0.2 mL replicates were inoculated with 2 μL of an overnight culture in a 96-well plate sealed with aluminum foil and grown anaerobically for 48 hr at 37°C. Samples were diluted 30,000-fold into buffer A (95% acetonitrile and 5% 100 mM ammonium formate). The concentration of d<sub>9</sub>-TMA in culture medium was determined using LC-MS. LC-MS/MS analysis was performed on an Agilent 6410 Triple Quadrupole LC/MS instrument (Agilent Technologies, Wilmington, DE). The LC analysis of d<sub>9</sub>-TMA was performed in positive mode, using a Kinetex (Phenomenex) HILIC column (2.6 μm, 30 mm × 2.1 mm, 100 Å), preceded by a SecurityGuard ULTRA Holder (Phenomenex). The LC conditions were: 0% B for 2.5 min, a gradient increasing to 100% B over 5 min, 100% B for 2.5 min, and 0% B for 2.5 min (solvent A = 95% acetonitrile and 5% 100 mM ammonium formate, solvent B = 50% acetonitrile, 40% water and 10% 50 mM ammonium formate). The flow rate was maintained at 0.8 ml/min for each run. Run time per sample was 12.5 min. The injection volume was 3 μL for both standards and samples. Samples and blanks were introduced via an electrospray ionization (ESI) source. The mass spectrometers were operated in multiple reaction monitoring (MRM) mode. The capillary voltage was set to 4.0 kV and the fragmentor voltage to 110 V. The drying gas temperature was maintained at 200°C with a flow rate of 10 l/min and a nebulizer pressure of 45 psi. The precursor-product ion pairs used in MRM mode were: m/z 69.1 → m/z 51. The collision energies for the precursor-product ion pairs were 21 V. MS1 and MS2 resolution was set to unit, the time filter width used was 0.07 min, and the ΔEMV (Electron Multiplier Voltage) was 400 V. Data analysis was performed with Mass Hunter Workstation Data Acquisition software (Agilent Technologies).

#### Community Profiling by Sequencing

Bacterial communities resulting from inoculation of germ-free animals were analyzed according to published methods (McNulty et al., 2011; Romano et al., 2015). DNA was extracted from cecal samples according to published bead-beating procedures (Turnbaugh et al., 2009). In short, fecal samples were resuspended in a solution containing 500 μL of 2X extraction buffer [200 mM Tris (pH 8.0), 200 mM NaCl, 20 mM EDTA], 210 μL of 20% SDS, 500 μL phenol:chloroform:isoamyl alcohol (pH 7.9, 25:24:1) and 500 μL of 0.1-mm diameter zirconia/silica beads. Cells were mechanically disrupted using a bead beater (BioSpec Products, Barlesville, OK) for 3 min at room temperature. The aqueous layer was removed and DNA precipitated using 600 μl isopropanol and 60 μl 3M



Na-acetate. Pellets were dried with ethanol and resuspended in TE. NucleoSpin Gel and PCR Clean-up Kit (Macherey-Nagel, Bethlehem, PA) was used to remove contaminants. Isolated DNA was stored at  $-80^{\circ}\text{C}$  until downstream processing.

Libraries were prepared according to a slightly modified version of the protocol accompanying the Illumina Genomic DNA Sample Prep Kit. Briefly, total bacterial gDNA was sonicated in 0.5 mL tubes in a BioRuptor XL water bath sonicator (Total Time: 20 min, Water Temp:  $4^{\circ}\text{C}$ , Power Setter: High, Time ON: 30 s, Time OFF: 30 s), cleaned up and concentrated using a Macherey-Nagel PCR Purification column. DNA was blunted and poly-A tailed. The A-tailed molecules were ligated to the relevant barcoded Illumina adaptor sequence. Adaptered-DNA was then size-selected ( $\sim 200$  bp) by agarose gel electrophoresis. Fragments of the appropriate size were PCR amplified and purified, after which the purified PCR products were given to the University of Wisconsin-Madison Biotechnology Center for quality assurance and library sequencing following the manufacturer's protocols. Sequences were demultiplexed by 7 bp barcode, requiring an exact match (sequences without a barcode match were excluded from the analysis). After demultiplexing, all sequences were trimmed to 35 bases to eliminate low-quality bases at the ends of each read and to allow for analysis using Bowtie as a part of the COPROseq pipeline ([https://github.com/DanishKhan14/aligner\\_RL](https://github.com/DanishKhan14/aligner_RL)). Sequences were aligned to the reference genomes of the 6 bacteria included in the study using Bowtie. Only reads which mapped uniquely to the reference genomes were used for abundance analysis. Raw counts were normalized based on the genome size of each organism included in the analysis. The proportional representation of each organism in the analysis was determined by dividing its normalized counts within a sample by the total normalized counts for all organisms within that sample.

### qRT-PCR

Primers used for qRT-PCR are listed in the [Table S2](#). cDNA was prepared using  $\sim 1$   $\mu\text{g}$  total RNA extracted as described below in the RNaseq subsection. 1  $\mu\text{l}$  cDNA was used in each 10  $\mu\text{l}$  SYBR Green (BioRad) reaction. Plates were run on a BioRad CFX96 instrument. Fold-change was calculated using standard Delta-Delta Ct calculations with  $\beta$ -actin as an internal control.

### RNaseq Library Prep

RNA was extracted from frozen livers by TRIzol extraction and then further cleaned using the QIAGEN RNeasy Mini Kit and quantified using a Nanodrop 2000 spectrophotometer. A single-end cDNA library was prepared using the Illumina TruSeq stranded mRNA Sample Preparation kit (RS-122-2101) according to the manufacturer's specifications and sequenced at the UW-Madison Biotechnology Center. Analysis details can be found below in [RNaseq Analysis](#).

### RNaseq Analysis

Samples were multiplexed, normalized, and pooled prior to sequencing on a HiSeq2000 at the University of Wisconsin-Madison Biotechnology Center. Sequencing reads were processed and filtered using the FastX Toolkit (Hannon Lab). The first 10 bp of each read were removed to eliminate GC bias at the beginning of each read using the FastX Trimmer. The 6 bp Illumina adaptor sequences were then clipped using the FastX Clipper and a quality filter was applied to eliminate any reads with a quality score  $< 30$  as determined by the FastX Quality Filter. Reads were then aligned to the mm9 mouse reference genome constructed to include only annotated genes (NM\_RefSeqs) by Bowtie2 alignment ([Langmead and Salzberg, 2012](#)). Seed length was set to 28 and allowed 2 mismatches per seed. Gene expression was then calculated using RSEM with a forward probability of 0.0 (for stranded libraries). Differential expression (DE) was calculated using EBSseq with a false discovery rate (FDR) = 0.1 ([Leng et al., 2013](#); [Li and Dewey, 2011](#)). DE genes were curated by hand for functional clustering analysis.

### Serum and Hepatic Metabolite Extraction

Serum samples used for TMAO and choline measurements were prepared for analysis by precipitating proteins with 4 volumes of ice-cold methanol spiked with 2.5  $\mu\text{M}$  deuterium-labeled choline and TMAO internal standards. Samples were centrifuged at 18,213  $\times g$  at  $4^{\circ}\text{C}$  for 3 min. The recovered supernatants were diluted 1:1 in uHPLC-grade water prior to screening. Serum samples for metabolome study were prepared by precipitating 50  $\mu\text{l}$  of serum with 4 volumes of ice-cold methanol. Precipitate solutions were kept at  $-20^{\circ}\text{C}$  for 20 min and then centrifuged at 18,000  $\times g$  for 10 min at  $4^{\circ}\text{C}$ . Supernatant was removed and the protein pellet was resuspended in 1 ml of 40:40:20 methanol:acetonitrile:water and allowed to incubate on ice for 10 min. The resuspension was centrifuged at 18,000  $\times g$  for 10 min at  $4^{\circ}\text{C}$  and the resulting supernatant pooled with the previously removed supernatant. Collected supernatant was dried under  $\text{N}_2$  gas and resuspended in 0.5 mL HPLC grade water. Hepatic metabolomes were extracted from 50 mg of homogenized tissue in 1 mL pre-chilled 80:20 methanol:water on dry ice for 5 min. Extractions were centrifuged at 18,000  $\times g$  for 5 min at  $4^{\circ}\text{C}$ . Supernatant was removed and the tissue pellet was resuspended in 0.8 mL of 40:40:20 methanol:acetonitrile:water and allowed to incubate on ice for 5 min. The resuspension was centrifuged at 18,000  $\times g$  for 5 min at  $4^{\circ}\text{C}$  and resulting supernatant was combined with the first extract. The extraction with 0.8 mL of 40:40:20 methanol:acetonitrile:water was repeated and combined with the pooled first and second extraction. Pooled extract was centrifuged at 18,000  $\times g$  for 5 min at  $4^{\circ}\text{C}$  to further remove any remaining insoluble particles. The supernatant was dried under  $\text{N}_2$  gas and resuspended in HPLC grade water at a ratio of 150  $\mu\text{l}/5$  mg tissue.

### uHPLC/MS/MS Metabolome Profiling

After sample preparation, identification and quantitation of TMAO and choline were performed using a uHPLC (Thermo Scientific/Dionex 3000) coupled to a high-resolution mass spectrometer (Thermo Scientific Q Exactive). Liquid chromatography separation was achieved on a Dikma Bio-Bond  $\text{C}_4$  column (150 mm by 2.1 mm; 3- $\mu\text{m}$  particle size) using a 7 min isocratic gradient (50:50 methanol

[MeOH]–water, 5 mM ammonium formate, and 0.1% formic acid). A heated electrospray ionization interface, working in positive mode, was used to direct column eluent to the mass spectrometer. Quantitation of TMAO and  $d_9$ -TMAO was performed via targeted MS/MS using the following paired masses of parent ions and fragments: TMAO (76.0762 and 58.0659) and  $d_9$ -TMAO (85.1318 and 68.1301). Quantitation of choline and  $d_9$ -choline was performed in full-MS scan mode by monitoring their exact masses: 104.1075 and 113.1631, respectively (Romano et al., 2015).

Serum and hepatic metabolomes were measured using a C18 method previously published (Pisithkul et al., 2015). Samples were analyzed using an HPLC-tandem MS (HPLC-MS/MS) system consisting of a Thermo Scientific/Dionex UHPLC coupled by electrospray ionization (ESI) (negative mode) to a hybrid quadrupole–high-resolution mass spectrometer (Q Exactive Orbitrap; Thermo Scientific) operated in full scan mode for detection of targeted compounds based on their accurate masses. Liquid chromatography (LC) separation was achieved using an Acquity UPLC BEH C18 column (2.1- by 100-mm column, 1.7- $\mu$ m particle size). Solvent A was 97:3 water:methanol with 10 mM tributylamine (TBA) and 10 mM acetic acid, pH 8.2; solvent B was 100% methanol. The total run time was 25 min with the following gradient: 0 min, 5% B; 2.5 min, 5% B; 5 min, 20% B; 7.5 min, 20% B; 13 min, 55% B; 15.5 min, 95% B; 18.5 min, 95% B; 19 min, 5% B; and 25 min, 5% B. Metabolite peaks were identified using the Metabolomics Analysis and Visualization Engine (MAVEN) (Melamud et al., 2010).

### Marble-Burying Assay

8-week old mice were placed in naive, freshly autoclaved cages with an array of 25 autoclaved marbles. After 30 min mice were removed and two independent investigators (one of them blinded to the treatment) determined the number of marbles buried  $\geq 50\%$ . Independent counts did not ever differ by more than 2 marbles. Cages were maintained in a biological safety cabinet for the duration of the experiment with visual barriers between replicate cages.

### Neonate sexing

Neonates were sexed using PCR. DNA was extracted from tail snips collected at the time of sacrifice by incubation at 98°C in 75  $\mu$ l of 25 mM NaOH/0.2 mM EDTA followed by the addition of 75  $\mu$ l of 40 mM Tris HCl (pH 5.5) (Wang and Storm, 2006). 1  $\mu$ l of total genomic DNA was amplified with the primers located in Table S2. PCR reactions were performed in a final volume of 25  $\mu$ l using GoTaq Green Master Mix (Promega) with 0.2  $\mu$ M of the above-mentioned primers. PCR parameters are as follows: initial denaturation at 94°C for 2 min, 35 cycles with 94°C for 30 s, 57°C for 30 s, and 72°C for 30 s, followed by final elongation at 72°C for 5 min. PCR products were visualized on a 2% agarose gel in 1X TAE with SYBR Safe DNA gel stain (Invitrogen) using the transillumination setting on the FOTO/Analyst FX (FotoDyne). Males were identified as having a single PCR product of 280 bp, females were identified as having two PCR products, one at 685 bp and the other at 480 bp (McFarlane et al., 2013).

### Hepatic Triglyceride Quantification

Liver TG was quantified following the Bligh and Dyer extraction method (Bligh and Dyer, 1959). 10–30 mg frozen liver tissue was homogenized in PBS (a 40  $\mu$ l of 1X PBS/mg tissue). An aliquot of homogenate was diluted (1:100) in water and 5  $\mu$ l used to measure protein using the Bradford Assay (BioRad; Cat.# 500-0201). 50  $\mu$ l of the remaining homogenate were mixed with 550  $\mu$ l of PBS and 3 mL of ice cold 2:1 MeOH:chloroform in a glass Hungate tube with Teflon lined screw cap. Tubes were vortexed vigorously for 1 min and then incubated overnight at  $-20^\circ\text{C}$ . 500  $\mu$ l ice-cold chloroform and 1 mL ice-cold water were added and tubes vortexed for 1 min. Organic and aqueous layers were separated and the bottom chloroform layer was transferred into a new tube. The organic extract was dried under  $\text{N}_2$ . 10  $\mu$ l of chloroform were added to the tubes and vortexed for 5 s before 90  $\mu$ l of 10% Triton X-100 (in 100% isopropanol) were added. Tubes were then vortexed for 5 s (or until no visible residue was left on the sides of the tubes). Lipid calibrator (Wako Lipid Calibrator; Cat.# 464-01601) was diluted with 1 mL of water. Standards for the calibration curve were made by mixing different volumes of the resuspended calibrator with 10  $\mu$ l chloroform, 24  $\mu$ l 37.5% Triton X-100 (in 100% isopropanol), and the corresponding volume of water to total 100  $\mu$ l. 50  $\mu$ l of each standard and sample was mixed with 900  $\mu$ l Wako R1 Type M (Wako R1 Type M; Cat.# 461-08992), vortexed, and incubated at 37°C for 5 min. After 5 min, 300  $\mu$ l Wako R2 Type M (Wako R1 Type M; Cat.# 461-09092) was added to each sample, vortexed, and incubated at 37°C for 5 min. Samples were vortexed until they looked clear. 200  $\mu$ l aliquots of each sample were transferred (triplicates) into a 96 well plate and the absorbance measured at 595nm. Triglyceride content was expressed as  $\mu\text{g}$  of TG per milligram of protein. Number of biological replicates is indicated in the respective figure legends.

### Serum Triglyceride Quantification

Serum TG were quantified using the L-type Triglyceride M kit from Wako Diagnostics (Richmond, VA) in line with manufacturer's instructions for microplate applications. In short, 12  $\mu$ l serum sample were mixed with 270  $\mu$ l Wako R1 Type M. Samples were vortexed and incubated at 37°C for 5 min. Following incubation 90  $\mu$ l of Wako R2 Type M was added and samples were vortexed and incubated at 37°C for 5 min. Samples were vortexed until clear. 115  $\mu$ l were pipetted in triplicate into a flat bottom 96-well plate and the absorbance measured at 595nm. Lipid calibrator was resuspended in water to a final concentration of 300 mg/dL and serially diluted to create standard curve. 12  $\mu$ l of each standard was processed as detailed above to create a standard curve. Number of biological replicates is indicated in respective figure legends.

### DNA Global Methylation Assay

Global methylation was measured using MethylFlash Global DNA Methylation ELISA Easy Kit from EpiGentek (Farmingdale, NY). DNA was extracted from tissue using the bead beating method detailed above. In short, tissue (half of the brain, ~25 mg of heart, ~100 mg of liver, and half of the distal colon) were suspended in a solution containing 500  $\mu$ L of 2X extraction buffer, 210  $\mu$ L of 20% SDS, 500  $\mu$ L phenol:chloroform:isoamyl alcohol, 500  $\mu$ L of 0.1-mm diameter zirconia/silica beads, and one 3.2-mm diameter stainless steel bead. Cells were mechanically disrupted using a bead beater for 3 min at room temperature. The aqueous layer (~450  $\mu$ L) was removed and DNA precipitated using 600  $\mu$ L isopropanol and 60  $\mu$ L 3M Na-acetate. Pellets were dried with ethanol and resuspended in TE. NucleoSpin Gel and PCR Clean-up Kit was used to remove contaminants. Isolated DNA was stored at  $-80^{\circ}\text{C}$  until downstream processing. DNA concentration was calculated using 3 replicate readings on the NanoDrop Spectrophotometer ND-100 (Thermo Fisher Scientific) and diluted to a final concentration of 100 ng/3  $\mu$ L. Using 100 ng (3  $\mu$ L) of diluted DNA, global 5mC was measured directly according to manufacturer's instructions provided with the kit. All standards were measured in duplicate while all samples were measured once due to well limitations in the ELISA plate. Number of biological replicates is indicated in the respective figure legends.

### Free Fatty Acids Assay

Serum FFA levels were measured using a colorimetric Free Fatty Acid Assay Kit (Cat. # STA-618) from Cell Biolabs (San Diego, CA) according to manufacturer's instructions provided with the kit. Briefly, flash frozen serum was diluted (1:10) in 1X Assay Buffer for the assay. 10  $\mu$ L of each sample and standard was then mixed with 200  $\mu$ L of 1X Enzyme Mixture A and incubated in a 96-well plate for 30 min at  $37^{\circ}\text{C}$  in the dark. After incubation, 100  $\mu$ L of the prepared Detection Enzyme Mixture were added and samples were incubated for 10 min at  $37^{\circ}\text{C}$  in the dark. Absorbance was measured at 540nm. Three technical replicates were run for each sample and standard. Number of biological replicates is indicated in the respective figure legends.

### Leptin Assay

Serum leptin levels were measured using the Leptin (mouse) ELISA Kit (Cat. # ADI-900-019A) from Enzo (Farmingdale, NY) according to manufacturer's instructions provided with the kit. Briefly, samples were diluted (1:32) in Assay Buffer. 100  $\mu$ L of each sample, standard, and blank were added to the ELISA plate (provided with the kit) and incubated for 1 hr with shaking at room-temperature. Wells were washed 3X and 100  $\mu$ L of antibody were added to each well (except blanks) and the plate was incubated for 1h with shaking at room-temperature. Following incubation, wells were washed 3X, 100  $\mu$ L of blue conjugate were added to each well (except the blank) and the plate was incubated for 30 min at room temperature with shaking. Following incubation, wells were washed 3X and 100  $\mu$ L of substrate solution was added to each well. The plate was incubated for 30 min with shaking at room temperature. After incubation, a 100  $\mu$ L aliquot of stop solution was added and absorbance measured at 450nm. All standards were measured in duplicate while all samples were measured once due to well limitations in the ELISA plate. Number of biological replicates is indicated in the respective figure legends.

### Community Profiling by 16S rRNA Gene Sequencing

Community composition was determined by amplicon sequencing of the variable 4 (V4) region of the 16S rRNA gene (Kozich et al., 2013) using the Illumina MiSeq platform (San Diego, CA). PCR was performed using primers for the variable 4 (V4) region of the bacterial 16S rRNA gene (Kozich et al., 2013). PCR reactions contained 12.5 ng DNA, 10  $\mu$ M of each primer, 12.5  $\mu$ L 2X HotStart ReadyMix (KAPA Biosystems, Wilmington, MA, USA), and water to 25  $\mu$ L. Cycling conditions were  $95^{\circ}\text{C}$  for 3 min, then 25 cycles of  $95^{\circ}\text{C}$  for 30 s,  $55^{\circ}\text{C}$  for 30 s, and  $72^{\circ}\text{C}$  for 30 s, and finally  $72^{\circ}\text{C}$  for 5 min. PCR products were purified by gel extraction from a 1% low-melt agarose gel using a ZR-96 Zymoclean Gel DNA Recovery Kit (Zymo Research, Irvine, CA). Individual samples were quantified by Qubit Fluorometer (Invitrogen, Carlsbad, CA, USA) and equimolar pooled. The pool plus 5% PhiX control DNA was sequenced with the MiSeq 2x250 v2 kit (Illumina, San Diego, CA, USA) using custom sequencing primers at the University of Wisconsin – Madison Biotechnology Center (Kozich et al., 2013). Sequences were analyzed in mothur (Schloss et al., 2009) following recommended procedures (Kozich et al., 2013). Sequences were clustered into 97% operational taxonomic units (OTUs) using OptiClust (Westcott and Schloss, 2017) and classified to a custom database containing the species used in this study: *Bacteroides caccae* (AAVM02000001), *Bacteroides ovatus* (AAXF02000018), *Bacteroides thetaiotaomicron* (AE015928), *Collinsella aerofaciens* (AAVN02000007), *Eubacterium rectale* (L34627), and a number of *Escherichia coli* MS strains as the strain used (MS 200-1) was not available (ADTK01000014, ADTL01000003, ADTP01000052, ADTR01000016, ADTX01000014, ADUA01000035, ADUG01000003, ADWQ01000120, ADWR01000036, ADWS01000032, ADWT01000015, ADWU01000043, ADWV01000069).

### QUANTIFICATION AND STATISTICAL ANALYSIS

The number of mice per group is indicated in corresponding figure legends. No formal sample-size estimation was performed. Number of mice used for different assays is based on previous experience and published literature. Significance was assessed using unpaired two-tailed Student's t test or ANOVA (as annotated in the corresponding figure legends) in GraphPad Prism. In all figures, the mean value is visually depicted  $\pm$  SEMs. P values correlate with symbols as follows: \*,  $p < 0.05$ ; \*\*,  $p < 0.01$ ; \*\*\*,  $p < 0.001$ ; \*\*\*\*,  $p < 0.0001$ . Mice were randomly assigned into experimental groups after matching for age and gender. Investigators remained unblinded

to group assignments throughout unless noted. Differential expression of genes was completed using EBseq as described in the “RNAseq analysis” subsection of Method Details. There were not subjects/data points excluded for statistical analyses/reporting.

#### **DATA AND SOFTWARE AVAILABILITY**

The accession number for RNA sequencing data at NCBI GEO is GEO: GSE100983. The accession numbers for COPROseq and 16S data, deposited to the Sequence Read Archive, are BioProject SRA: PRJNA393700 and BioSamples SRA: SAMN07346941, SAMN07346942, SAMN07346943, SAMN07346944, SAMN07346945, SAMN07346946, SAMN07346947, SAMN07346948, SAMN07346949, SAMN07346950, SAMN07346951, SAMN07346952, SAMN07346953, SAMN07346954, SAMN07346955, SAMN07346956, SAMN07346957, SAMN07346958, SAMN07346959, SAMN07346960, SAMN07346961, and SAMN07346962. COPROseq Pipeline can be found at [https://github.com/DanishKhan14/aligner\\_RL](https://github.com/DanishKhan14/aligner_RL).